Progress In Electromagnetics Research, Vol. 171, 89–121, 2021

Reconfigurable Antennas: A Review of Recent Progress and Future Prospects for Next Generation

Ryan J. Beneck*, Arkaprovo Das, Galestan Mackertich-Sengerdy, Ryan J. Chaky, Yuhao Wu, Saber Soltani, and Douglas H. Werner

(*Invited Paper*)

Abstract—Reconfigurable antennas are devices that can dynamically alter their geometry and/or electromagnetic properties to facilitate different behaviors. Numerous approaches for achieving reconfigurability have been studied over the past 20 years, mainly consisting of mechanical, electrical, optical, and metamaterial methods. This review presents the most notable works and advancements in this field while placing a significant focus on antennas with explicit practical applications in the emerging areas of millimeter waves, 5G/6G communications, Internet-of-Things (IoT), high-throughput satellites, and miniaturized systems among several others. The various reconfiguration methods mentioned will be compared, and their benefits and drawbacks discussed.

1. INTRODUCTION

The broad subject of Reconfigurable Systems [1–6] has garnered significant attention over the last few decades and has been a topic of active research in the recent past. Reconfigurable antennas [7] constitute an extensive segment of reconfigurable systems aimed at achieving reconfigurability primarily at the RF, microwave and millimeter-wave regimes of the frequency spectrum. With technology trends and applications such as 5G communications, Internet-of-Things (IoT), autonomous vehicles, integrated space and terrestrial networks gaining prominence, the need for developing novel and cutting-edge design technologies to achieve reconfigurability in antenna systems is even more necessitated. This review article is directed towards furnishing the readers with a perspective of recent advancements in the field of reconfigurable antennas, the technological innovations that demonstrate reconfigurable characteristics, the latest growth trends and traction in this discipline and the authors' standpoint on futuristic prospects of technologies that could be implemented into commercialized applications. It is noteworthy that there have been several review papers published previously on reconfigurable antennas. However, a significant number of new and innovative developments have been reported since these papers first appeared. This review article therefore focuses mainly on providing a summary of significant recent developments in the field as well as some insights into the future prospects for next generation systems.

Reconfigurable antennas are antennas or an array of antenna elements that can dynamically achieve a reversible alteration of operating frequency, radiation-pattern properties, polarization modes, bandwidth characteristics or a combination of a few or all of these aspects to suit a specific application. These antennas have a major advantage of being multi-functional in nature, which subsequently reduces the number of antennas required and hence the total occupied footprint for performing multiple specific objectives. Frequency reconfigurable antennas can dynamically tune-in to different frequencies of

Received 11 August 2021, Accepted 11 October 2021, Scheduled 16 October 2021
* Corresponding author: Ryan J. Beneck (rbeneck95@gmail.com).
The authors are with the Computational Electromagnetics and Antennas Research Laboratory (CEARL) at The Pennsylvania State University, USA.

operation, thereby alleviating the need to design multi-band antenna systems. Pattern reconfigurable antennas can steer the main radiation beam, place nulls at intended angular locations, and alter the pattern shape, directivity, and gain of the antennas depending on the applications they cater to. This contrasts with the smart and adaptive antenna technology where the adaptive beam switching operation is largely dependent on an external beam-forming network instead of an internally equipped tuning mechanism. Polarization reconfigurable antennas on the other hand can switch between different polarization states, for example — switch from a vertically polarized pattern to a circularly polarized one. This multi-functional trait of reconfigurable antennas has attracted a lot of interest over the last few years. Figure 1 shows the growth in the number of technical articles published in IEEE journals and conference proceedings since 2000.

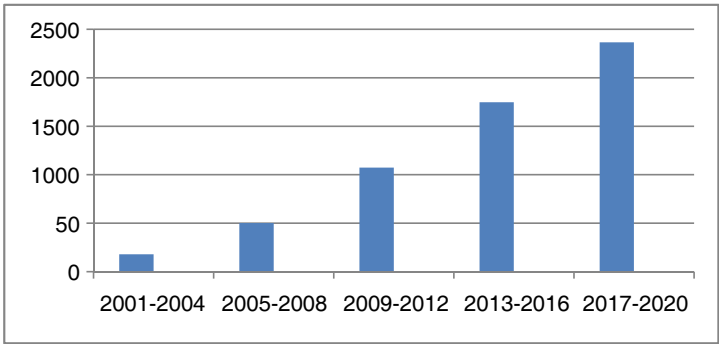

Figure 1. Bar chart representing the growth of IEEE publications related to "Reconfigurable Antennas" over the last 20 years.

Reconfigurability in an antenna system is generally achieved by dynamically modifying the path traversed by the currents on the structure or by changing the antenna's effective aperture. Additionally, for an array of antenna elements, this is traditionally accomplished by customizing the amplitude and phase excitations of the individual radiators. There are a plethora of techniques described in the literature that aid in realizing the aforementioned objectives. The most popular electrical approach among them is to incorporate RF micro-electromechanical systems (MEMS) and active switches in the antenna design configuration [8–11], which subsequently generates a dynamic switching response to effectively change the current distribution. Recently, artificially engineered materials such as metamaterials and metasurfaces have been demonstrated to be effective in obtaining reconfigurable and tunable characteristics for antenna applications [2]. Alternatively, switching mechanism can also be triggered by invoking optically induced phenomena such as photoconductive effects [12], Optically Induced Plasmas (OIP), etc. Furthermore, mechanical reconfigurability of several parts of the antenna system can also result in tunable electrical characteristics [7]. Figure 2 depicts different methods and technologies used for achieving antenna reconfiguration. The work is broadly classified into 4 sub-categories: mechanical, electrical, optical and metamaterial methods.

The remainder of the paper describes each of the reconfiguration methods in further detail. Section 2 highlights the mechanical methods that have been employed for reconfiguration. Although not sorted according to priority, mechanical methods being the oldest option have been placed on the top of the list. Section 3 enumerates the pros and cons of several electrical technologies to achieve reconfiguration, while optically induced reconfiguration mechanisms are explained in Section 4. Section 5 outlines the role of artificially engineered materials such as metamaterials, metasurfaces and frequency selective surfaces in obtaining reconfigurable characteristics, with emphasis on space and next generation terrestrial applications. Section 6 concludes the paper with notes on future prospects.

2. MECHANICAL METHODS

One of the first reconfigurable antennas consisted of the integration of mechanical components into the antenna's operation. In 1935 a rhombic antenna radiation pattern was altered by adjusting

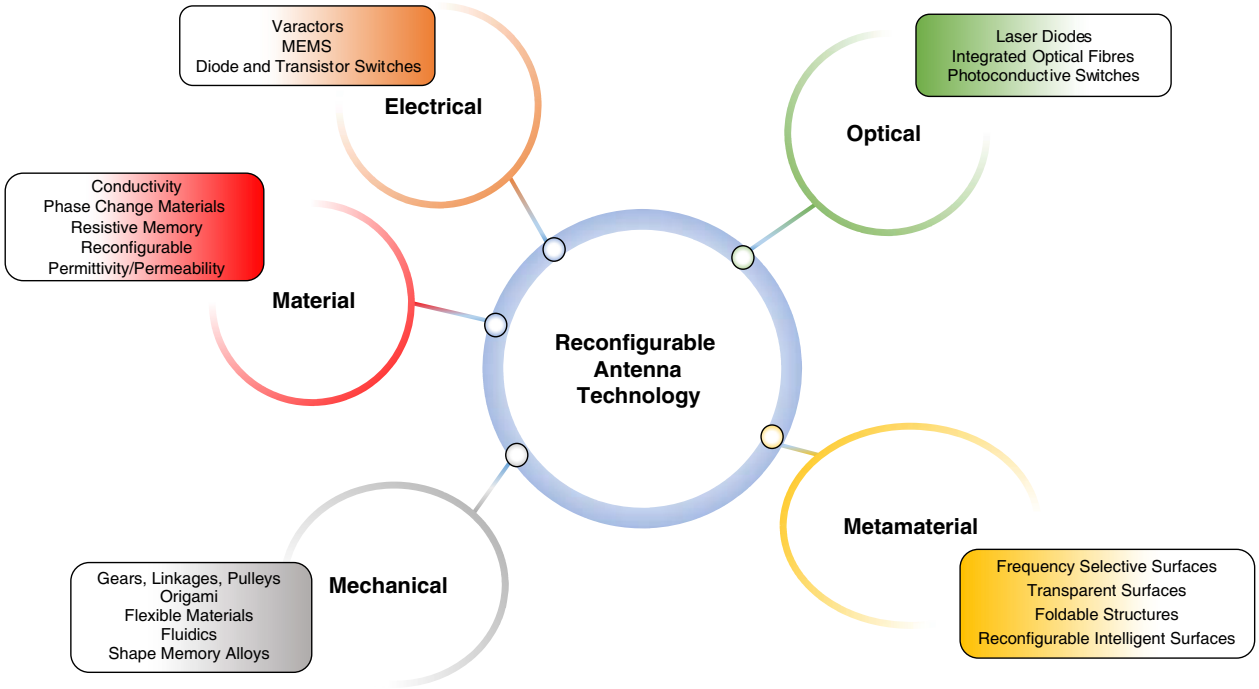

Figure 2. Visual summary of the broad classification of different methods to achieve reconfiguration.

counterweights changing the inclusion angle of the wire elements [13]. One of the most famous applications of mechanical methods is the Gregorian dome and carriage house of the Aricebo observatory [7]. Recently, there have been advancements in the mechanical methods such as the implementation of dielectric fluid loaded antennas, conductive fluid antennas, gearing and linkage systems, and origami-based antennas.

Some of the most popular mechanical based antennas are the gear/linkage-based systems. These are antennas or antenna systems that consist of a rotating/translating layer that can alter the operating frequency [14, 15], steer the resultant beam to the desired direction [16–19], create ultrawideband or stopband frequency operation [20] or change the resultant polarization [21, 22]. Another method to introduce reconfiguration can be achieved by implementing origami techniques. Origami (the art of paper folding) has similar reconfiguration capabilities such as the polarization and/or frequency reconfiguration [23, 24]. However, utilizing the art of origami, antennas can be stored or transported as flat sheets (reducing total package size) and when they reach their application destination, are folded/unfolded into the operational shape [25, 26]. The shape modification for reconfiguration is not limited to strictly origami methods. The lamination of asymmetric glass fibers into the substrate and activating springs fabricated from Ni/Ti shape memory causes the substrate to deform into 2 differing shapes. This mechanical reconfiguration method allows the resultant beam to be steered to two differing angles [27]. Figure 3 shows an origami segmented helix antenna with reconfigurable polarization.

An interesting application of a mechanically reconfigurable antenna is the high gain slotted waveguide with a simple rotating shutter system for 5G applications (shown in Figure 4). It demonstrates that even at the higher 5G frequencies a robust and simple mechanical solution is achievable.

Some of the more interesting applications of mechanical based reconfiguration methods are their implementation into high-power systems. As presented by Campbell et al., mechanical methods used with a 2D unit-cell and then later a 3D unit-cell (shown in Figure 5) can achieve a target reflection phase angle behavior under high power microwave conditions [28]. This solution was then demonstrated by the successful completion of a fabricated prototype [29]. Some other mechanical reconfiguration methods applied to high power applications involve the modification of the half-power beamwidth (HPBW) of a horn antenna by changing the location of metal flaps [30]. This method was successful in changing the

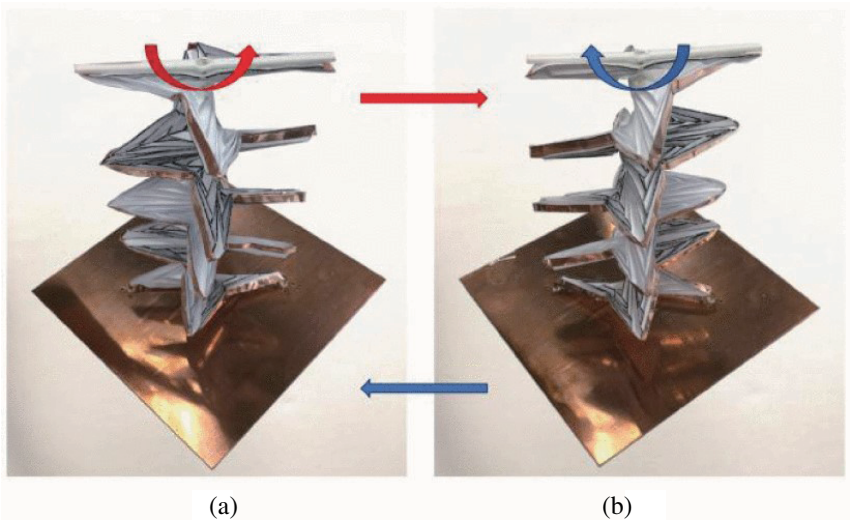

(a) (b)

Figure 3. Segmented helix antenna fabricated using origami methods. (a) Left-handed state. (b) Right-handed state. © 2018 IEEE. Reprinted, with permission, from [23].

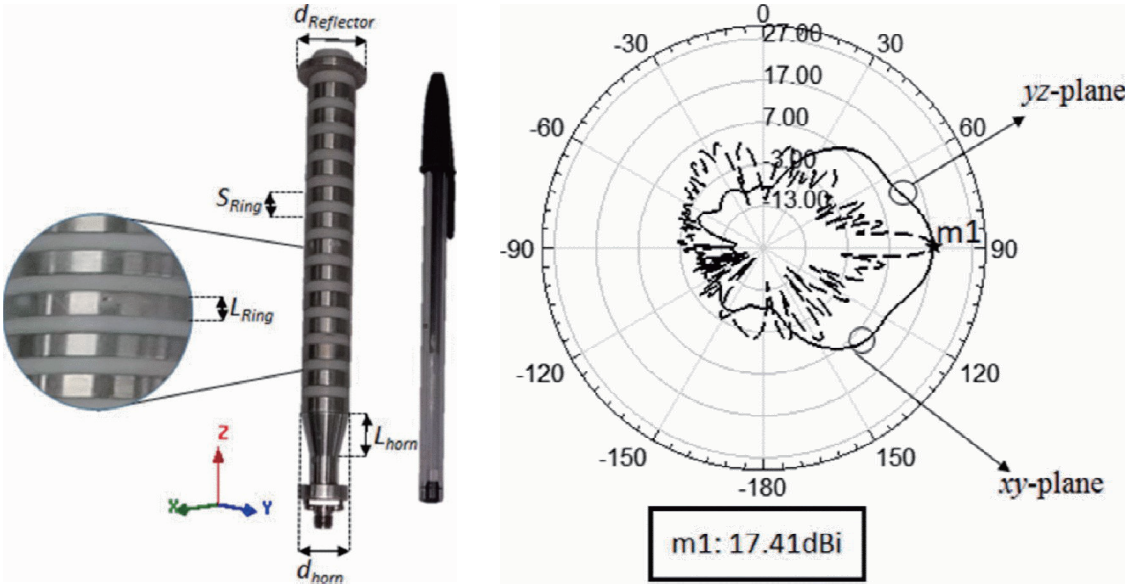

(a) (b)

Figure 4. (a) Omnidirectional ring based slotted waveguide array as fabricated. (b) Radiation pattern mechanically configured array at 27.3 GHz with 17.4 dBi of realized gain. © 2017 IEEE. Reprinted, with permission, from [17].

HPBW from 58.7 to 16.5 degrees.

Fluidic devices are another interesting class of antennas that achieve reconfigurability by adjusting the fluid level within a device to create a reconfigurable resonant chamber. This is done by either adjusting the fluid composition and channels, or by having shaped fluid filled containers to achieve novel performance. These antennas can use pure water, sea water, ionic liquids, room-temperature liquid metals, colloidal dispersions in dielectric oils or various other liquids [3, 31–37].

The mechanical methods that are described above are just a small sub-set of all the existing mechanical methods used for reconfiguration. There are several other mechanical methods that are

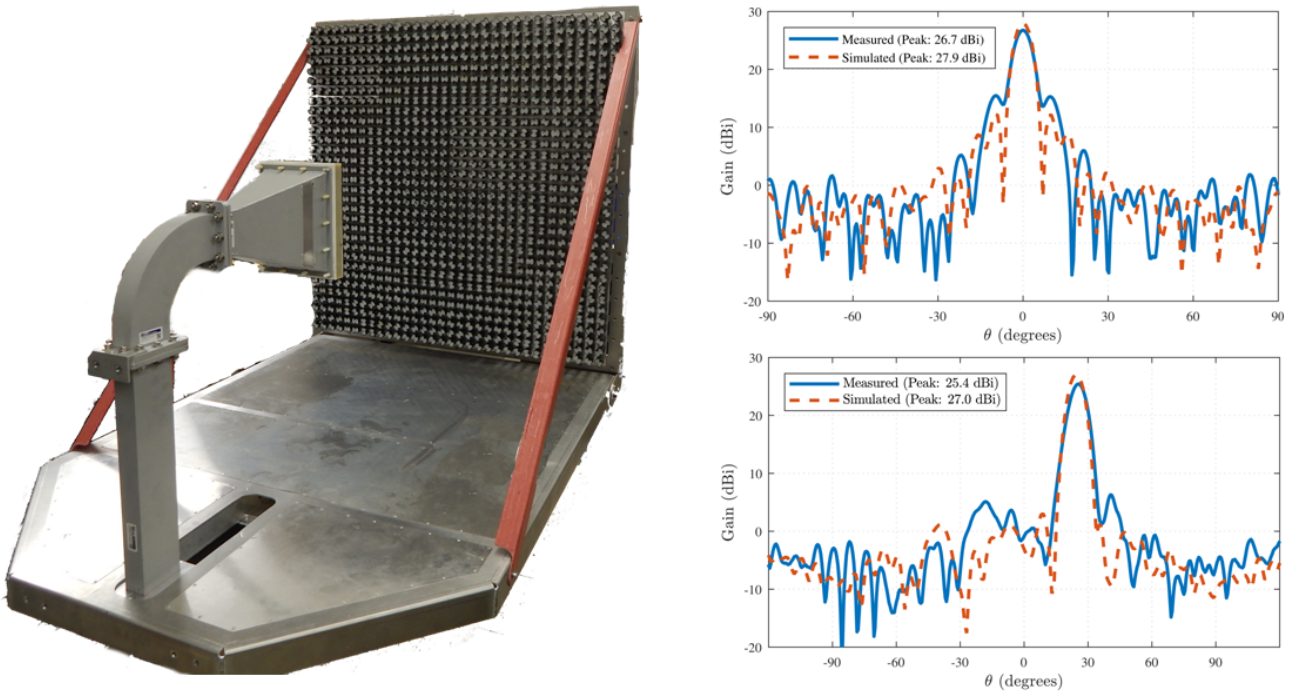

(a) (b)

Figure 5. (a) Fabricated and assembled mechanically reconfigurable metamaterial enabled high power antenna. (b) Simulated and measured far-field gain patterns for broadside and steered configurations. © 2020 IEEE. Reprinted, with permission, from [29].

available for 5G and future communication applications. These include physically deforming the parabolic reflector surface using flexible materials and liquid-metals to stretch and fold the antenna to achieve reconfiguration, and textile-based antennas that are frequency reconfigurable [38–40].

3. ELECTRICAL METHODS

The electrical techniques used for actuating reconfiguration in antennas are broadly dependent on effective switching mechanisms. This can be realized either by using electronic and mechanical switches such as PIN diodes, MEMS switches, etc. or by effectively altering the constituent properties of materials. Subsections 3.1–3.3 illustrate several electronic and electro-mechanical switches used for the purpose. On the other hand, the use of material properties for achieving reconfiguration is detailed in Subsections 3.4–3.7.

3.1. Conventional Diode and Transistor Switches

The most common electronic switching technique is the usage of PIN diodes due to its affordability, excellent power handling capability, scalability, prolonged lifetime, simple control, compactness, ease of fabrication for optimal results, higher switching speed in the orders of nanoseconds, and reliability [41–43]. As the control current is varied between the HIGH and LOW states, these diodes facilitate switching, pulse modulation, phase shift and attenuation of the radio frequency signals [44]. However, the PIN switches suffer from a few disadvantages due to their non-linearity, lower isolation, high power losses and high insertion losses [41–43]. The insertion loss in these switches was found to be in between 0.4 and 0.7 dB [45]. With increasing number of PIN diodes in the system, the biasing circuitry becomes increasingly complicated, and the insertion loss considerably increases [45].

On the other hand, GaAs FET switches exhibit higher switching speeds, better isolation properties, lesser insertion losses, compact sizes, lower power consumption, easier integration with the antenna

systems, lower assembly cost and low ON state resistances [43]. FET switches, unlike PIN diodes, do not need RF chokes in their biasing networks. As the biasing technique is simpler, the FET switches exhibit no adverse effects in the pattern, gain and efficiency of the antenna. CMOS switches exhibit high power handling capabilities, easier integration into the antenna design and easier control. Even for higher voltage amplitudes, the CMOS switches exhibit a linear response. However, a smaller number of tuning states can only be realized with these switches [46]. Figure 6 depicts the top and bottom views of a reconfigurable antenna for 2.5 GHz operation. Here the reconfiguration is affected by using PIN diodes as switches. Recently, many reconfigurable antennas using PIN diodes as switches have been reported for frequency [47, 48], pattern [48–51], and polarization [48, 51] reconfiguration.

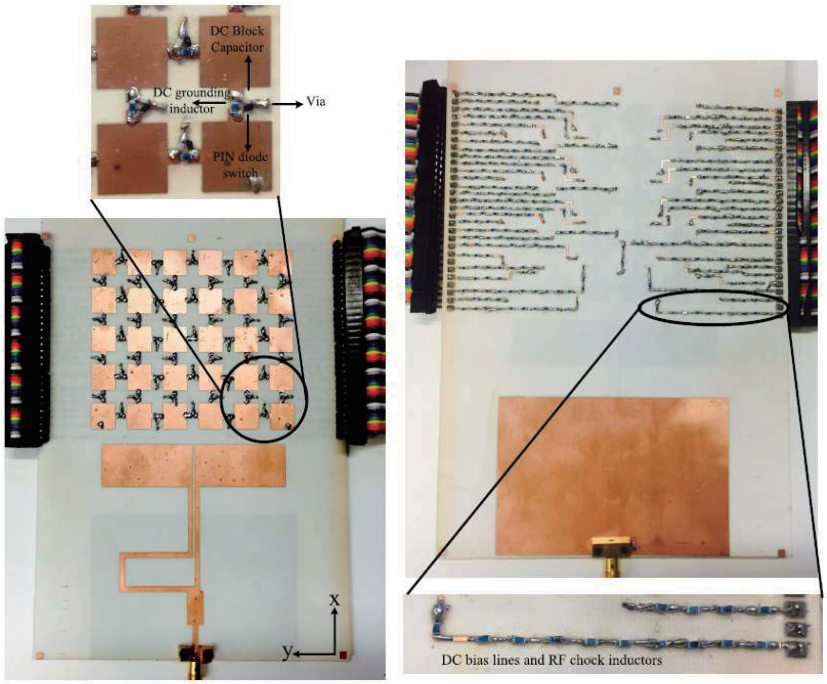

Figure 6. Reconfigurable antenna for 2.5 GHz operation: (a) Photograph of the top view. Inset: switch structure. (b) Photograph of the bottom view. Inset: dc bias lines. © 2017 IEEE. Reprinted, with permission, from [46].

3.2. Varactor Switches and Tuned Capacitances

Varactors are voltage-controlled capacitors with fast switching speeds and can be easily integrated into antenna circuitry due to their smaller sizes [42, 52]. Varactors are used for fast and easier tuning and provide a broader tuning range [52]. These devices are compact, readily available commercially, and low-priced. As varactor diode switches are operated using reverse bias voltages, a lower current consumption is required as compared to PIN and MEMS switches for their activation, thus resulting in lower power consumption [53]. A minimum number of varactor switches can provide multiple modes with more flexibility [53]. On the flip side, the use of varactors for reconfiguration purposes is hindered by their nonlinear response and high voltage requirements [42]. Figure 7 below shows the use of varactor diodes in conjunction with a metasurface-based Artificial Magnetic Conductor (AMC) to miniaturize a planar crossed end-loaded dipole (ELD) antenna [54, 55]. This strategy enables the operation of the tuned antenna over a frequency range of one to two octaves as well as facilitates a reconfigurable polarization.

In a similar context, there has been a substantial amount of literature that refers to the use of switchable capacitances for achieving reconfigurability. This is traditionally attained by using lumped capacitor components, while other methods of generating the capacitance values are also reported.

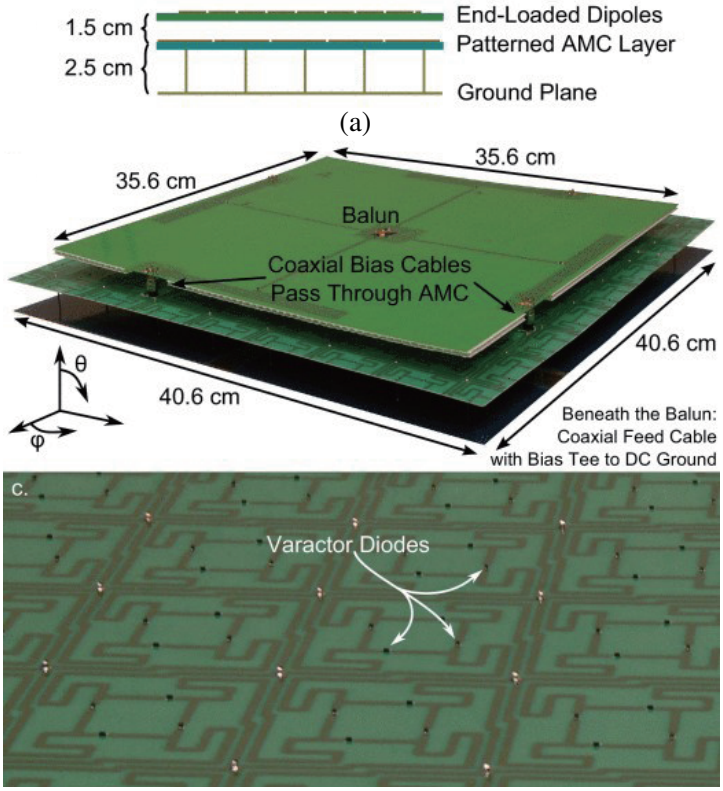

Figure 7. Antenna geometry and photographs. (a) Side-view schematic of the antenna. The thickness from the ground plane to the ELDs is 4 cm, while the total antenna thickness approaches 4.5 cm when including circuit components on both the top and bottom circuit boards. (b) Photographs showing the details of antenna and the tunable AMC. © 2016 IEEE. Reprinted, with permission, from [54].

It is noteworthy to mention that the use of switchable capacitances can accomplish reconfigurability for both resonant and leaky-wave antennas (LWA). LWAs are antennas that leak radiation from the structure when a guided-wave mode propagates through them. This property of LWAs enables beam-steering capabilities as the frequency is varied. Although the steering angle of the main lobe depends on the propagation constant of the propagating mode, β, a lack of control of the main beam can still stem from the non-linear dependence of β on frequency due to dispersion. Furthermore, for band-limited systems, the maximum allowable frequency bandwidth might be restricted while the scanning coverage desired is wider. In those cases, dependence on frequency of operation to achieve beam-steering capabilities can severely hinder the scan coverage of the antenna. These factors necessitate the need for developing LWAs equipped with a potential for reconfiguration that can steer the main-beam at a fixed frequency of interest, a technique also known as 'fixed-frequency beam scanning'. It has been shown in [56] that the propagation constant β can also be altered at a fixed frequency by changing the admittance of the radiating wall of the LWA. Exploiting this property, the work in [57] proposes genetic-algorithm optimized switch configurations that optimally switch between 35 equally-spaced 0.2 pF capacitors loading a reconfigurable half-width microstrip LWA to achieve beam-steering. *Suntives and Hum* in [58, 59] make use of a series-shunt configuration of lumped capacitors to alter the wall admittance of the LWA. Deviating from the usage of traditional passive lumped elements, the recent work in [60] uses a PIN-diode to switch ON/OFF two gap-coupled capacitances loading a half-width microstrip LWA. This double-gap capacitor technique enabled the antenna prototype to scan the main beam forward between $+28^\circ$ and $+67^\circ$ and backward between -27° and -66° at 4.2 GHz.

3.3. MEMS Switches

MEMS switches are traditionally limited in terms of packaging, reliability and power handling capabilities [8, 9]. These switches exhibit a slower response and a lower tunable range as compared to their PIN diode and varactor counterparts. Whereas, compared to the discrete components' integration into the antenna design, monolithic fabrication of antenna and switches together minimizes the losses and parasitic effects [41]. Furthermore, MEMS switches require complex matching networks [42]. They also need additional voltage upconverter chips of 30 to 90 V conversion levels if used in portable communication devices. The process of assembling these switches into Printed Circuit Boards (PCBs) is reportedly difficult. The requirement of higher voltages for activation is another disadvantage of MEMS switches which makes them less reliable for practical use [41–43]. In [10], a parasitic layer-based multifunctional reconfigurable antenna (MRA) with an interconnecting MEMS switch is presented, as shown in Figure 8. The antenna tunes its operating polarization/radiation pattern according to switch combinations. In recent years, examples of reconfigurable spiral-shaped monopole antennas [61], concentric ring structured reconfigurable antennas [62] and frequency reconfigurable antennas [63] using MEMS switches have also been demonstrated.

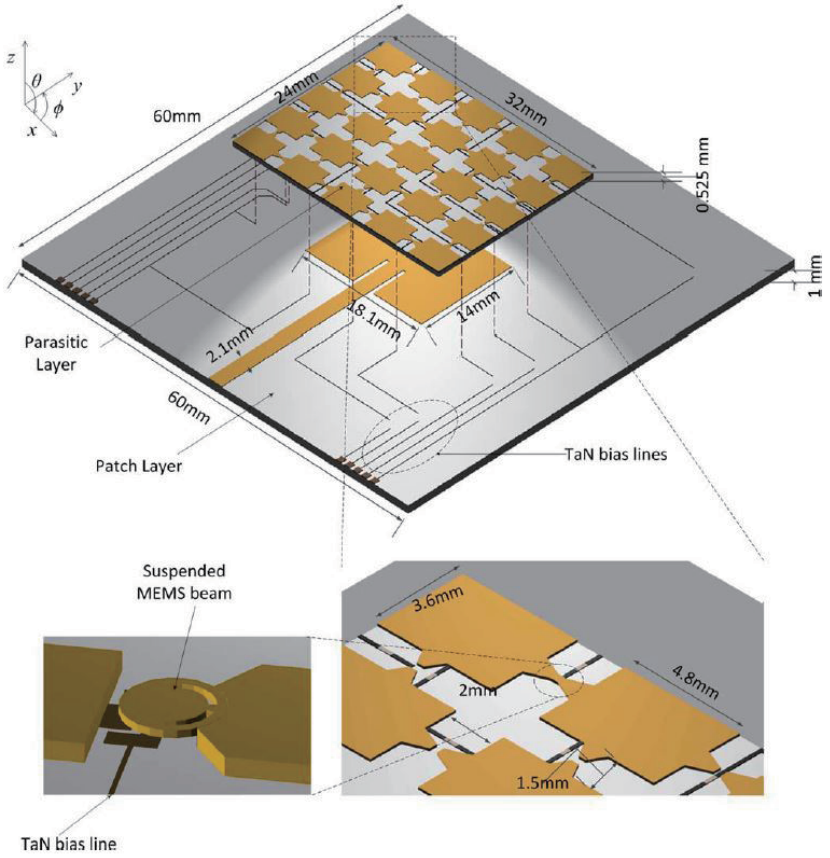

Figure 8. Three-dimensional schematic of the "MRA parasitic" with a magnified view of adjacent pixels and an interconnecting MEMS switch (for the sake of illustration, the parasitic layer is suspended on top of the patch layer). © 2012 IEEE. Reprinted, with permission, from [10].

In general, the installation of electrical switching components within antenna structures increases the circuit intricacies and enhanced losses since these switches use biasing connections for activation. This phenomenon adversely affects the radiation pattern of the antenna [42]. In this context, it is noteworthy to explain some designs which are least affected by the above mentioned issues. In many recently reported works, DC bias lines are not required for several novel geometries that employ MEMS switches. This results in easier fabrication and improved radiation patterns as any leakage loss or

coupling loss with the bias lines can be readily mitigated. In some designs, the biasing circuit is integrated into the antenna plane for PIN diodes without any vias, which in turn reduces the losses associated with bias lines [11]. FET switches can also be activated by a digital signal without requiring a DC bias or biasing networks as reported in [43].

3.4. Resistive Memory and Memristors

Memristors and resistive memory devices can change their resistances based on external stimuli [64, 65]. Notably, they are both passive and require no additional energy to maintain a resistance state once reached [66]. Memristors are sometimes combined with other circuit elements and can be used in the design of tunable filters which are commonly implemented to switch between band-pass and band-stop modes. The operation of these filters in band-pass mode allows a signal to be better received in low noise situations, while band-stop mode eliminates unnecessary signals in noisy environments. These filters are therefore a popular choice for use in 5G applications. Although tunable filters predominantly consist of conventional active devices such as transistors, relays, PIN diodes, or MEMS, the use of memristors for this purpose consumes less energy and has better performance potential compared to traditional devices [67, 68]. Two examples of reconfigurable devices that incorporate memristors are shown in Figure 9 below.

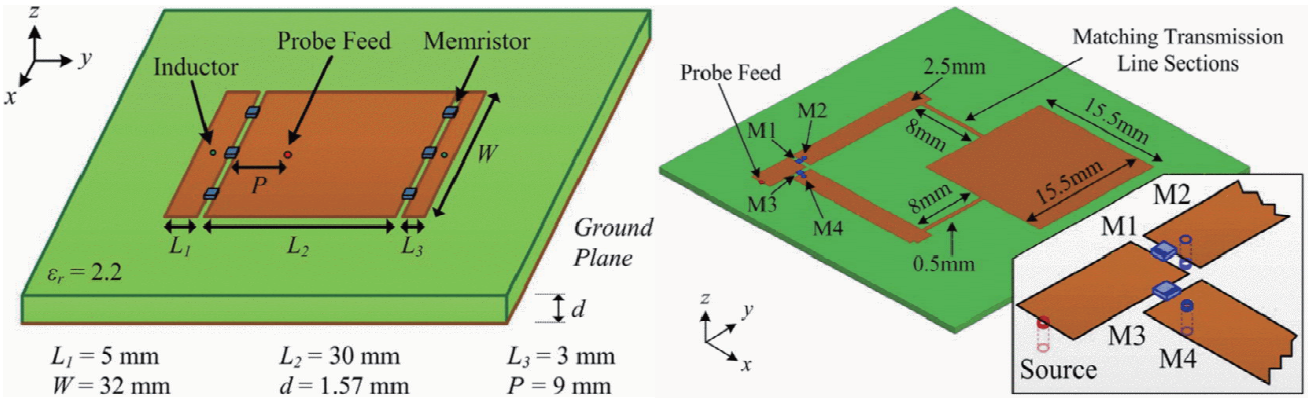

(a) (b)

Figure 9. (a) Diagram of a memristor-enabled reconfigurable band-switching antenna. (b) Diagram of a polarization reconfigurable patch antenna containing memristors. © 2015 IEEE. Reprinted, with permission, from [65].

A simulated tunable filter consisting of a memristor, varactors, and a stub-loaded stepped-impedance resonator is presented in [69]. A tuning range from 3.4 GHz to 3.6 GHz was achieved, which fits into one of the mid-band 5G spectra. This design was not fabricated, and a material for the memristor was not chosen. However, the authors see great potential in this setup for use in future 5G systems. Nevertheless, memristive switches are not only limited to this frequency range. As reported in [70], nanoscale memristive switches have demonstrated operation from 10 GHz to 40 GHz. This nanoscale design was fabricated on a silicon wafer with thermally grown silicon dioxide. Other materials used in construction were gold, titanium, and silver. This device's frequency range includes many millimeter wave bands of the 5G spectrum, and the researchers emphasize that this technology will likely become prominent in future consumer electronics and RF circuit applications. An example of one of these nanoscale switches is shown in Figure 10 below.

Another form of resistive memory switch derives from 2D materials and is known as an atomristor. 2D materials, such as graphene and h-BN (hexagonal boron-nitride) are structures which are a single atom in thickness and have useful material properties. Many of these 2D materials have been shown to have non-volatile resistance switching (NVRS) properties. The works in [71] and [72] show examples of atomristor RF switches which are operational up to 50 GHz and 100 GHz respectively, and thus includes

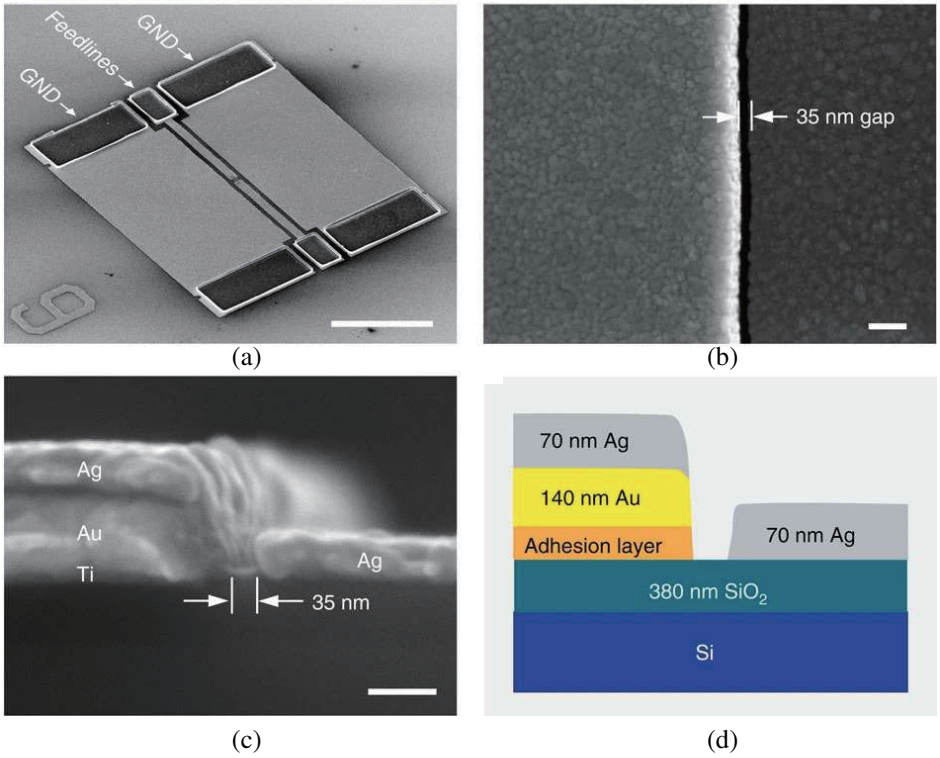

Figure 10. (a) Nanoscale memristive RF switch. (b) Top view of air gap. (c) Cross-sectional view of air gap and electrodes. (d) Diagram showing geometry of the device and the materials used. Reprinted by permission from Springer Nature Customer Service Centre GmbH: Springer Nature, Nature Communications [70] © 2015.

several bands in the 5G millimeter wave spectrum.

Resistive memory-based RF switches have potential for use in future 5G and X-band systems. This newer technology has numerous performance benefits over older devices. While these switches are yet to become commonplace, many researchers in this field see the potential of resistive memory as important components of future 5G and X-band reconfigurable antennas.

3.5. Phase Change Materials (PCM)

In the past two decades, various research groups have focused on developing multifunctional RF devices. Phase Change Materials (PCMs), which provide an extra freedom of tunability, have become an inevitable choice besides the more conventional temporal and spatial modification techniques. PCMs have been used to design devices for X-band applications rather than 5G. One example presents a reconfigurable bandpass filter with an uplink frequency range of 7.9–8.4 GHz and a downlink range of 7.25–7.75 GHz [73]. However, it does suffer from issues of reliability and robustness. A second example demonstrates a laser-excited RF switch [74]. As a third example, PCM based switches have been utilized in coupled microstrip lines to achieve similar functionality [73]. In these three cases, the phase change material used is Germanium telluride (GeTe).

Vanadium dioxide (VO_2) is a popular phase changing material capable of going through a fast and reversible phase transition. At a critical temperature of 341 K, it can transition from a semi-conductor to a metallic state. The change in optical properties in PCMs is accentuated by the transition between two crystalline states — the monoclinic structure below the critical temperature and the tetragonal structure above the critical temperature. By taking advantage of the fast response speed of the PCM, high frequency RF, millimeter wave and photonic devices have been proposed with dual or even multiple functionalities. In [75], a laser deposited VO_2 based reversible RF-microwave switch was experimentally

proven by researchers, which has a potential for use in various tunable high frequency communication devices. The switches were investigated with both shunt and series configurations, which proved to have 30–40 dB isolation from 500 MHz to 35 GHz and a 2.5 dB loss when operating in the ON-state. In 2014 [76], a single-pole single-throw (SPST) VO_2 based millimeter wave switch was proposed with low insertion loss (0.2 dB in the ON-state) and high isolation (21 dB in the OFF-state). The device reached a 40 THz cut-off frequency with a low off-capacitance of 4 fF and a low power budget (2 V, 8 mA), which enables high-performance millimeter FPGA operation. In 2015, a low loss (0.13 dB at 50 GHz, 0.5 dB at 110 GHz) VO_2 millimeter wave switch with a 45 THz cut-off frequency was proposed, which can operate up to the W-band spectrum [77]. The same group also reported an SPST configured series switch that has < 1 dB insertion loss and > 12 dB isolation at 220 GHz, which is suitable for millimeter and sub-millimeter wave applications [78]. Another notable work combined a thin VO_2 film with a nanoscale metal resonator to create a versatile multifunctional platform capable of computer control [79]. This approach can serve as a basis for creating future reconfigurable intelligent nanophotonic systems. As a proof of concept, the researchers used this method to create a hybrid metamaterial absorber (Figure 11) and for infrared camouflage. In [80–82], researchers demonstrated for the first time a VO_2-ink-printed, thermally controlled reconfigurable mechanism on a custom silver-organo-complex (SOC) ink supported flexible Kapton substrate, which was experimentally validated using antenna and switch configurations (PIFA, CPW switch) for different frequency ranges (Figure 12 shown below).

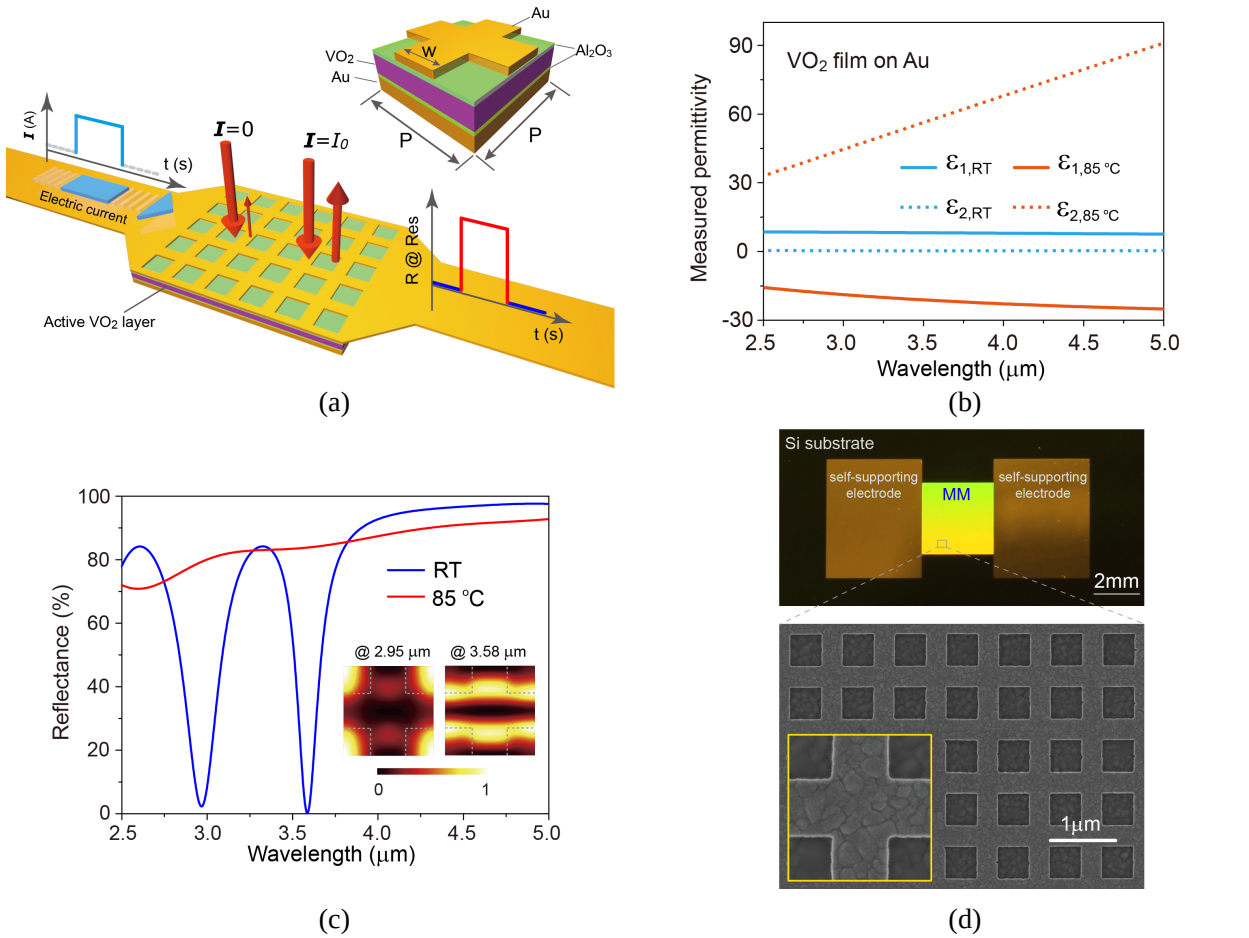

Figure 11. (a) Diagram of metamaterial absorber with gold (Au) and VO_2 layers. (b) Permittivity of VO_2 at different temperatures. (c) Simulated Reflectance of the absorber. (d) Photo of the absorber from an electron microscope. [79] © Liu et al. 2016, licensed under CC BY 4.0. http://creativecommons.org/licenses/by/4.0/.

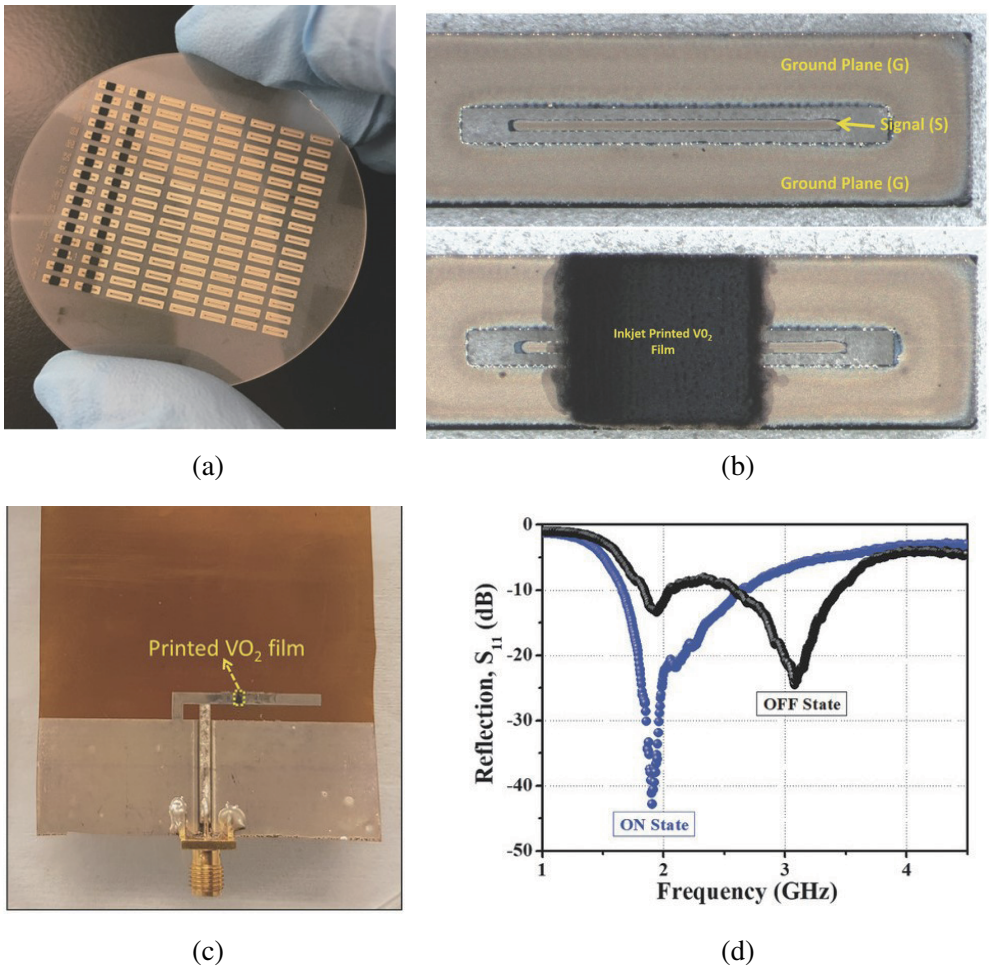

Figure 12. (a) Photo of fabricated series and shunt switches on Sapphire wafer. (b) Microscopic images of inkjet-printed CPW structure for shunt switches and inkjet-printed VO_2 film on top of printed CPW structure. (c) Fabricated prototype of the VO_2-based PIFA antenna. (d) The measured reflection coefficient of the antenna with the VO_2 switches in the ON/OFF state in flat condition. Adapted from [81] © 2018 WILEY-VCH Verlag GmbH & Co. KGaA, Weinheim.

Another class of PCMs that recently attracted tremendous attention in the RF community is chalcogenides, such as GeTe (Germanium Telluride), and GeSbTe (Germanium-Antimony-Tellurium or GST). The tunability of this class of PCM is induced by the transition between the crystalline state and the amorphous state, either electrically or thermally. Similar to VO_2, these materials also demonstrate a critical temperature, on either side of which they exhibit a significant change in their electromagnetic properties. These PCMs are widely implemented in photonic devices. A GeTe reconfigurable RF switch was achieved with low ON resistance (180 Ohms) and large dynamic range (over 7000 times) [83] under a 5 ns rise time for the electrical pulse excitation. In [84–86], a three-terminal and a 7 THz-cutoff four-terminal topology for the RF switches were exploited to realize a high OFF/ON resistance contrast, 50 Ohm/3.5 kOhm and 1.2 Ohm/113 kOhm, respectively. In these two configurations, the phase change from a conductive crystalline state to a high resistance amorphous state is induced by an external current ($\sim$ 10 mA) and an external voltage pulse modulation. In [87], a 12.5 THz cut-off inline phase change switch (IPCS) is realized with two configurations — single-pole single-throw (SPST) and single-pole double-throw (SPDT). The proposed IPCSs are designed with a significantly low on-resistance (0.9 Ohm) and off-capacitance (14.1 fF), which cumulatively contribute to a high cut-off frequency.

Meanwhile, in addition to the ON/OFF state resistances as described above, some researchers

have emphasized different Figures of Merit (FoM) including but not limited to thermal budget, response speed, stability, 1 dB compression point, etc. In [88], researchers modeled and experimentally characterized the critical RF and thermal specifications such as Joule's heating simulation, third order intercept point, response speed and 1 dB compression point (P1 dB) of the GeTe based RF switches. They reported a crystallization switch of 20 µs and an amorphous switch of 500 ns, while the P1 dB of the switch was around 20 dBm, which provides a superior performance to traditional MEMS-based switches in terms of switching speed and integration density. Another characterization of the GeTe based RF active elements was conducted in [89], where the optimized device was demonstrated to have a wideband low resistance (1.8 Ohm) in the ON-state and a low-profile of 300 nm thickness. In general, the device is capable of a large OFF/ON contrast of 1.8×10^4 with a 0.2 dB insertion loss up-to 40 GHz. Moreover, the GeTe switches were first fabricated with a lateral FET configuration in series and shunt fashion [90, 91]. This switch also has an insertion loss of < 0.2 dB and an isolation of 30 dB up to 67 GHz. A GeTe RF switch for operation at 11 THz was designed and tested under W-CDMA signals. An insertion loss of 0.25 dB and an isolation of 24 dB was reported with a 50-µm-wide device at 20 GHz [92]. A thermal stability analysis and the dependence of ON-state power handling capability of GeTe RF switches on the number of conditioning cycles has been studied in [73]. It has been shown that the power handling of a GeTe switch, thermally actuated by a tungsten heating mechanism can be increased by ~ 2 dB if the device is continually cycled over time for a few cycles. Furthermore, a low power budget GeTe based RF switch was designed with a CMOS integration process, which has a cut-off frequency of 22 THz and performs up to 65 GHz with large on-off contrast [93]. In 2018, SbTe was introduced as a new chalcogenide material, and the alloy was utilized in the construction of an RF switch. It was then fabricated on a TiW (Titanium Tungsten) heater substrate in a planar configuration, and this setup yielded a high FoM [94].

3.6. Reconfigurable Permittivity and Permeability Materials

Dynamic adjustments in the permittivity and/or permeability of a material alter the effective electrical dimensions (e.g., length) of an electromagnetic structure such as an antenna, which results in a shift in the frequency of operation [4]. This concept has been predominantly used to design reconfigurable antennas. There are different types of materials that can be used for this purpose and depending on the choice; a different stimulus or method is needed to modify their constituent properties.

Ferroelectric (FE) materials, with high dielectric constant and large tunability are widely utilized in the design of memory, sensors, actuators, and MEMS devices. The electromagnetic reconfigurability in FE materials stems from the external biasing field, the application of which can change the constitutive parameters. Due to their smaller footprint and low power budget, planar RF applications with FE composites, such as FE antennas [95], have been proposed over the past two decades. Furthermore, some FE materials with oxide doping, e.g., PSTO (lead strontium titanate oxide) and BSTO (barium strontium titanate oxide), maintain a relatively high dielectric constant while suppressing the loss tangent, which makes them even more suitable for high frequency RF applications. In 2001 [95], researchers first realized a 2D beam scanning capability across 20–60 GHz by integrating the low-loss ferroelectric material, BSTO, into the circularly arranged transverse stub design (CTS). The material that was chosen had a low loss tangent of 0.0009 and a high dielectric contrast (permittivity) tuning range of 19.81% (416.4–333.91). Another ferroelectric based single frequency scanning LWA [96] was proposed based on the transverse equivalent networks model, where the conductive superstrate of a slot array was used as both the partial reflective plane and the biased electrode. A screen-printed barium-strontium-titanate (BST) based phase-shifter antenna array operating at 10 GHz was designed with 100° of scanning range and a relatively high FoM [97]. By integrating a tunable BST layer, researchers realized a shifter configured for left-handed operation and associated bias circuitry with a fully planar configuration while not sacrificing the high FoM, $> 52°$/dB. Similarly, a compact screen-printed BST RF phase shifter was demonstrated with a high FoM of 45°/dB and a large phase shift range of 330° from 8.5 GHz to 13 GHz, which also makes use of the left-handed configuration [98]. In recent years, alternative FE materials have been investigated. In 2021, Aspe et al. implemented interdigitated varactors based on $K_{0.5}Na_{0.5}NbO_3$ material to create a frequency-tunable slot-loop antenna [99]. There has also been interest in the FE material lead magnesium niobate — lead titante for use in reconfigurable systems [100].

Liquid Crystal (LC) [5] is another good candidate for reconfigurable antenna technology due to its ability to tune the dielectric constant of the material [101]. A 3%–30% [102–104] permittivity variation ratio at different frequency ranges has been achieved by using LC. Also, LCs can be tuned thermally and electrically between all their various crystal phases. Previously, the potential of LC to realize reconfigurable devices has been investigated only in the optical region [105–109]. Its usage is more preferable at higher frequencies, predominantly over 30 GHz, because of its lower loss tangent, which makes it more competitive for 5G or millimeter-wave applications. In [110], a 5 GHz microstrip antenna with an LC substrate was proposed with a tri-layer Taconic TLY-5 substrate architecture. It realizes an impedance matching and broadside radiation performance from 5.75 GHz at 0 V bias to 5.3 GHz at 10 V bias, resulting in an 8% tunability range. In 2015, an LC based reconfigurable reflectarray antenna with a beam scanning range of 55° at 96–104 GHz was proposed that achieved a side lobe level of −13 dB across the angular range [111]. A novel shape-memory-polymer, liquid crystal elastomer (LCE), was used as an antenna substrate to enable tunability under a temperature change [112]. A k15 LC substrate antenna was compared with a conventional RT/Duroid 5880 substrate antenna, which outperforms the conventional counterpart with a bandwidth of 6.43%, a tuning range of 3.1% and a peak radiation efficiency of 70% [113]. In 2018, a differential probe-fed LC based frequency tunable circular ring patch antenna was proposed [114], in which the cavity model was utilized to analyze the differential operation and extract the permittivity of the tunable substrate.

LCs can also be used in reconfigurable LWAs [115]. The most common approach is to incorporate liquid crystals into a corrugated substrate integrated waveguide. These waveguides consist of a dielectric sandwiched between two metal plates, and then the plates are connected with vias or metal posts. Many works use a folded (or half-wave) version of this waveguide to reduce its physical size [116]. Then, by changing the bias voltage on the liquid crystals, effects such as beam steering can be achieved.

One of the more recent areas of research that can be potentially exploited for reconfigurable antenna applications is smart materials [117, 118]. Most of the designs in this category make use of a hollow substrate which can be filled with liquid. The ratio of air to liquid inside the substrate can be adjusted accordingly to modify the permittivity and/or permeability. Different liquids can be used, such as water or certain types of oils. Other designs of this type use substrates with multiple separate cavities which can contain the liquid. A reconfigurable monopole with an omnidirectional radiation pattern was created using this method, and it is able to operate at four different frequency bands [119]. Additionally, Chen et al. demonstrated a circularly polarized design [120]. In this antenna, liquid dielectric can be injected into different areas of the substrate and thus change the CP radiation from right-handed to left-handed and vice-versa. An example of a smart material antenna is shown in Figure 13.

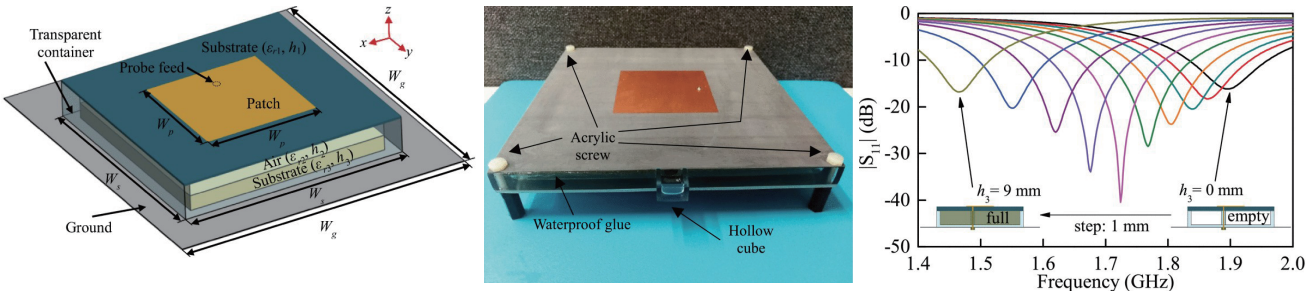

Figure 13. (a) Diagram showing layers of smart material enabled patch antenna system. (b) Fabricated example. (c) Reflection coefficient versus frequency for different oil levels. © 2017 IEEE. Reprinted, with permission, from [118].

3.7. Dielectric Gratings

A dielectric waveguide with periodic surface corrugations behaves as an LWA. These periodic corrugations excite a periodic disturbance of waves propagating through the uniform (non-perturbed)

portion of the waveguide, thereby causing leaky wave radiation [121]. This property of surface perturbation has been used over the years to design different configurations of dielectric LWAs. For example, Hammad et al. in [122] demonstrated a ground-backed dielectric grating antenna, developed using alumina as the antenna substrate and aluminum titanate as the grating material. The high permittivity of the grating material results in a higher leakage constant, which facilitates a considerable antenna size reduction. Additionally, the effects of different grating profiles including isosceles trapezoid, isosceles triangle, right-angled triangle, etc. are also studied. In another work [123], a supercell-based dielectric grating LWA is proposed for operation at 60 GHz. The antenna can simultaneously excite two spatial harmonic modes thereby resulting in two radiating beams in the far-field. However, none of these designs are equipped with reconfiguration capabilities.

Recently, to attain reconfigurability, a graphene LWA based on a dielectric grating was proposed in [124, 125]. The antenna is designed to be operational at the terahertz band of the frequency spectrum. In this set of works, the Surface Plasmon Polariton (SPP) propagating along the graphene surface as a slow-wave is made to leak radiation in free-space by the introduction of a dielectric grating structure. Furthermore, the fixed frequency beam reconfigurability is achieved by changing the biasing voltage applied to the grapheme sheet, and hence by changing its chemical potential.

Interestingly, Hu et al. in 2014 [126] demonstrated a reconfigurable LWA based on a periodic water grating housed on a grounded glass slab. The static configuration of water exhibits a large beam-scanning angle, while the dynamic configuration displays its tuning or reconfiguration capabilities. The dynamic configuration is achieved by properly controlling water flow among grooves. Using this technique, the main beam can be tuned from $-32°$ to $+18°$ at 5.5 GHz. Figure 14 shows the structure of the fabricated static LWA.

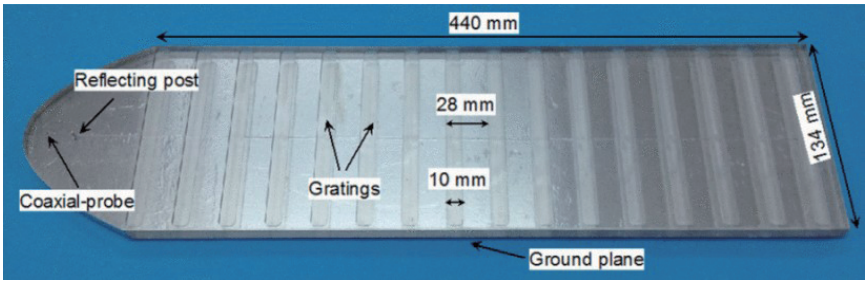

Figure 14. Photograph of static water grating LWA. © 2014 IEEE. Reprinted, with permission, from [126].

4. OPTICAL METHODS

Optical switches or optically excited photoconductive switches offer an alternate approach for reconfiguring antennas and other electromagnetic devices. These switches make use of the photoconductive effect inherent in semiconductors, whereby incident light with energy greater than the band gap of the semiconductor is absorbed, thus exciting electrons to the conduction band and resulting in the generation of electron-hole pairs. This generation of additional free charge carriers in the material results in an increase in the conductance around a localized region where the light is incident. The resultant change in conductivity may be described as a modification of both the static and alternating conductivity due to the time-varying incident optical field [12, 127].

A simple example of the most common type of photoconductive switch (PS) is shown in Figure 15(a). This type of PS is generally applied in PCB designs and consists of a silicon die adhered to the substrate within a gap in the transmission line or antenna. Often, a silver-loaded epoxy is used to improve the connection of the PS with the surrounding metallic elements [12]. A basic RC model of the switch is shown in Figure 15(b). As the optical intensity is increased, the resistance will decrease leading to an improved insertion loss. The resistance can also be further improved by increasing the field's penetration depth into the semiconductor material. Although it appears intuitive that decreasing

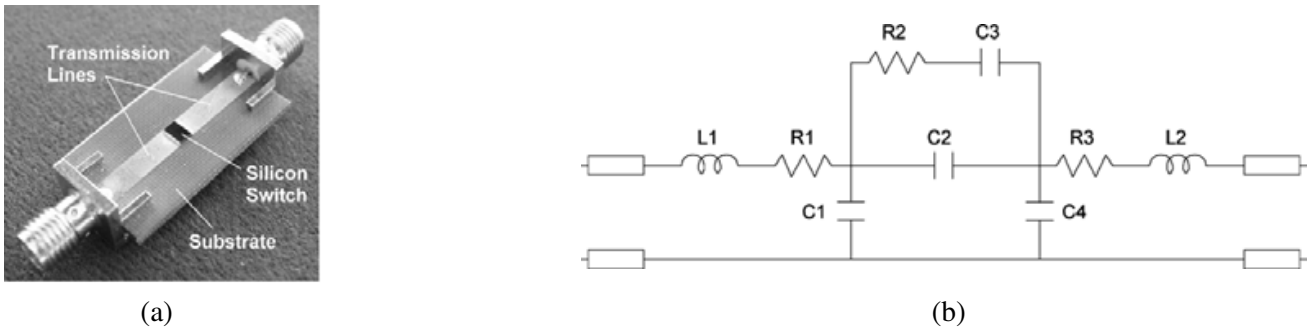

(a) (b)

Figure 15. (a) Geometry of a simple silicon photoconductive switch. (b) Equivalent circuit model. © 2006 IEEE. Reprinted, with permission, from [12].

the length of the switch would consequently improve the switch performance, capacitive coupling begins to dominate which in turn reduces the off-state isolation of the switch [128]. Thus, there is a noticeable and important tradeoff between acceptable insertion loss and state isolation that must be considered when using an optical switch. One of the primary advantages of using a PS instead of other alternatives is the electromagnetic isolation between optical and RF fields provided by this method. Considering that only an optical source is required to trigger the switch, no complex bias network is needed. As a result, the switches will neither introduce any nonlinear harmonics nor interfere with the outgoing radiation through undesirable coupling effects. Additionally, the PCs have been reported to exhibit switching times within the microseconds range [5, 129].

The development of optically reconfigurable antennas and similar electromagnetic devices can be grouped into different categories based upon how the PS is integrated within the device: a) integration within the radiating element, b) integration within a load or feeding network, and c) as a barrier to outgoing waves in the case of slotted antennas. The following paragraphs will summarize the work in each of these categories with a specific focus on the advantages and disadvantages of the various approaches, especially with regards to the real-world deployment of future telecommunications technologies.

The first approach focuses on the integration of one or more PS within the radiating element. An early implementation of this method was employed by the authors in [12]. In this work, a set of PS were added symmetrically to the arms of a coplanar dipole antenna. By applying incident light delivered with an optical fiber, the PS may be turned on and off resulting in a change in the antenna's electrical length with a corresponding shift in the resonant frequency. Since this class of designs includes the switch within the radiating element, material losses due to finite conductivity in the switch become more noticeable. In this case, the authors noted that it was necessary to increase the laser output power from 20 mW up to 200 mW in order to recover the reported 1 dB gain loss. Depending upon the desired application, this tradeoff may be nonnegotiable due to power and thermal dissipation requirements. Another similar work showed that as the optical power is increased, both the conductivity and the dielectric loss tangent of silicon will increase [130]. Thus, using higher optical powers to excite the switch is undesirable due to these added losses. In order to limit the effect of losses in the main radiating elements, the optical switch can instead be connected to a parasitic. In [128], the authors showed that the pattern could be reconfigured at a single frequency by tuning the phasing between two radiating patches as a result of a reconfigurable PS placed within the parasitic element. Given that the parasitic element, by nature, is located further away from the higher energy feed, the paper demonstrated that their goal could be retained using a low optical power of 30 mW.

An alternative and less expensive, albeit physically larger, approach to illuminate the PS uses integrated laser diodes in place of an off-board laser source and optical fibers. This is the approach undertaken in [131]. The diode is mounted on a copper plate directly behind the ground plane and holes are drilled into this plate and substrate in order to allow the light to pass through to the PS. This is shown in Figure 16(b). The copper plate also serves as a necessary heat sink which is able to improve the lifetime of the laser diode. Due to its larger physical size, direct integration using this method is likely to only be a viable solution for the Sub-6 band as opposed to mm-wave. However, this does not exclude the possibility of using this as an on-board light source, with optical fibers employed to guide

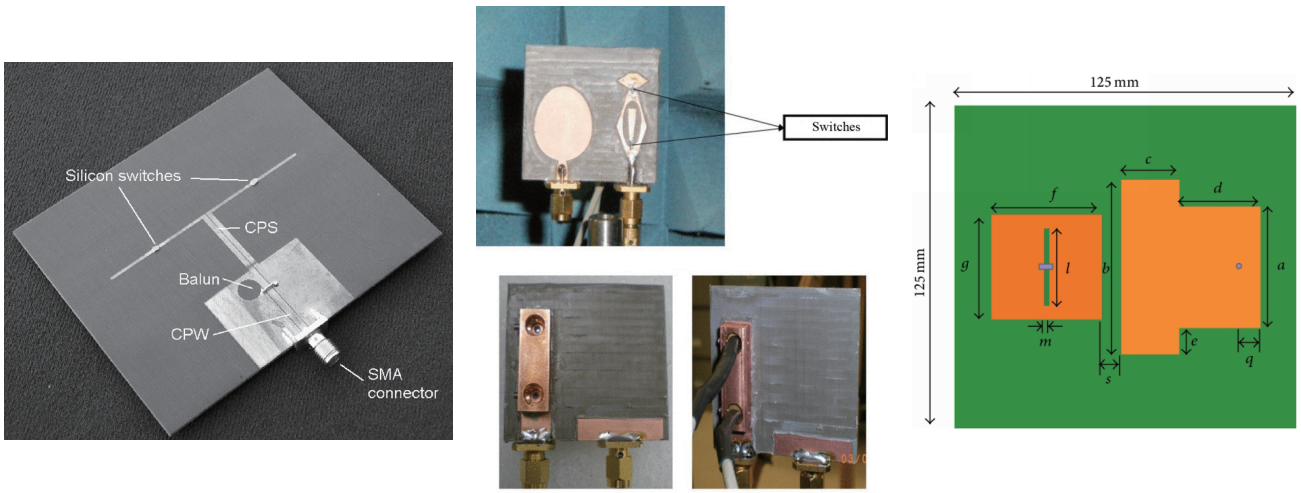

(a) (b) (c)

Figure 16. Sample of different designs integrating the PS within the radiating element. (a) © 2006 IEEE. Reprinted, with permission, from [12]. (b) © 2012 IEEE. Reprinted, with permission, from [131]. (c) © 2014 Deshuang Zhao et al. Reprinted from [132], licensed under CC BY 4.0. http://creativecommons.org/licenses/by/4.0/.

the light directly to the PS. For the study in [131], the authors demonstrated a cognitive radio system comprising an elliptic patch for the ultra-wideband (UWB) spectrum sensing component along with a modified printed monopole with two PS's as the reconfigurable antenna. The reconfigurable component is capable of being tuned over three different bands within the S- and C-bands.

The second category of studies on optically reconfigured antennas involves placing the PS within a load or the feed network. An initial study in [128] demonstrated the design of an optically controlled reconfigurable filter by tuning transmission line stubs. However, the final performance was degraded under low optical power. To alleviate this problem, another work by the same authors in [133] provides a promising solution by using a shorting stub in place of the more conventional open stub in order to reconfigure a patch antenna (Figure 17(a)). This modification enabled a large tuning range with lower optical power. The work by Silva et al. integrated SMD capacitors with the PS in order to realize a more complex filtenna (i.e., filtering antenna) design [134]. Furthermore, a PS was integrated into the probe feed of a patch antenna in [135]. More recently a stacked patch for 1-bit phase shifting at 24 GHz was demonstrated in [136]. The PS were controlled by integrating a simple PCB containing 100 mW LED's into the design. Though this wattage is higher than others discussed above, the LED integration is promising in comparison to many of the designs requiring a coherent laser source. This patch antenna is shown in Figure 17(b). As an alternative to laser sources, red, white, and violet LED's may also be used as a sufficient light source while operating in the Sub-6 band [137]. It is suggested here that LED's could become a more viable replacement option to laser excitation if lenses are also integrated into the system in order to focus the energy onto the PS.

Lastly for this section, a novel type of optically controlled antenna that does not use the conventional silicon die PS was studied in [138] (Figure 17(c)). The authors opted to use all off-the-shelf phototransistors and diodes in this work. The phototransistor acts as an optically controlled current source that will turn on or off the PIN diode by altering its bias voltage. An RF bias tee, connected to the RF input port, for the components is also added which renders the reconfigurable design as solely optically controlled. Remarkably, the paper indicated that a 0.3 dB insertion loss and 10 dB isolation was obtainable using only a 20 mW laser source per switch. The paper also illustrated a successful demonstration of a 2×2 array that could find application in a MIMO system due to the antennas 5 reconfigurable modes. Though the design was built for S-band, future work is expected to focus on similar design concepts in the mm-wave band due to the potential for a low-loss switching mechanism and use of off-the-shelf components.

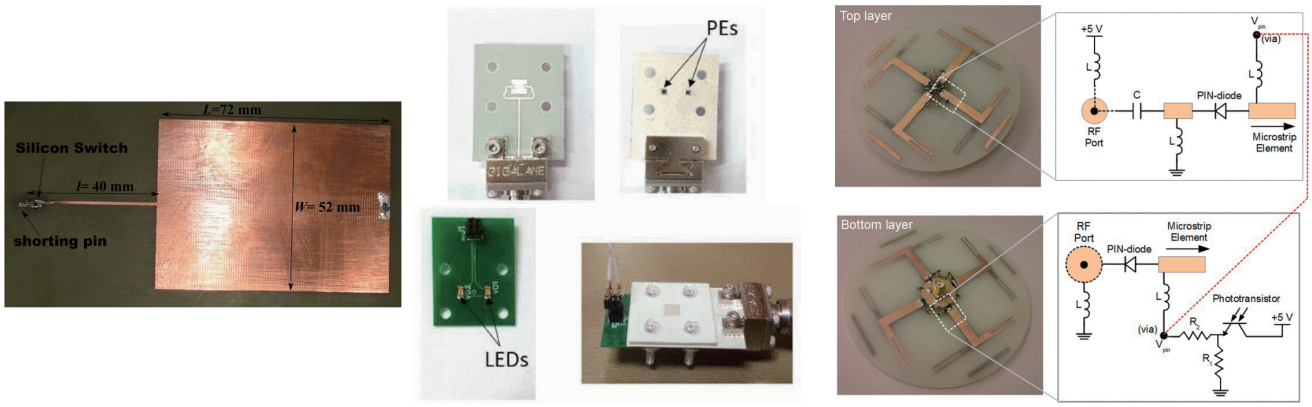

(a) (b) (c)

Figure 17. Sample of different designs isolating the PS from the radiating element. (a) © 2014 IEEE. Reprinted, with permission, from [133]. (b) © 2019 IEEE. Reprinted, with permission, from [136]. (c) © 2014 IEEE. Reprinted, with permission, from [138].

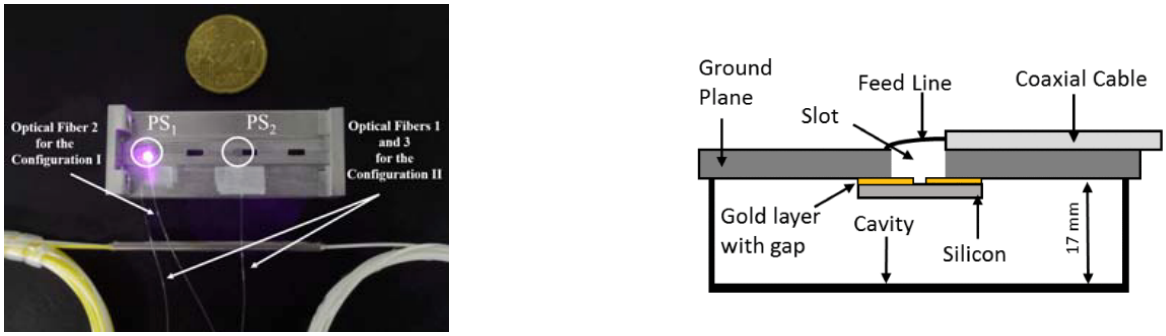

(a) (b)

Figure 18. Sample of different designs that include PS within the apertures in order to alter the radiation mode. (a) © 2017 IEEE. Reprinted, with permission, from [140]. (b) © 2017 IEEE. Reprinted, with permission, from [143].

Finally, the third category comprises slot antennas that include PS within the apertures in order to alter the radiation mode. The advantage in this case is that the PS is generally located further away from the high field intensity regions near the feed. A design based on a slotted circular waveguide antenna was investigated in [139]. By turning on or off different PS, the individual slots can be detuned resulting in a multi-state sectoral pattern depending on the state of each of the slots. The design is promising, yet it fails to address practical concerns associated with properly exciting each of the switches. The same authors, in a series of works [140–142], investigated a similar design, based on a rectangular slotted waveguide array (Figure 18(a)). Notably, the proposed device is able to reconfigure between the 28 GHz and 38 GHz bands by activating a set of PS located atop the slots. In this series of work, a successful implementation of a 64-bit quadrature amplitude modulation (64-QAM) scheme with photonic down conversion was also proven. Further, the work discussed the effect of the incident optical power on system-level diagnostics, such as the SNR, EVM (error vector magnitude), and MER (modulation error ratio). Unfortunately, adequate performance was not achieved until the optical power reached close to 1 W. Nevertheless, these papers are an important step in the direction towards the development of solutions specifically for next-generation telecommunications bands. Around the same time another group of researchers in [143] studied the application of PS within a cavity-backed slot antenna in the Sub-6 band. A diagram of this setup is shown in Figure 18(b). The switch design in this case, requires

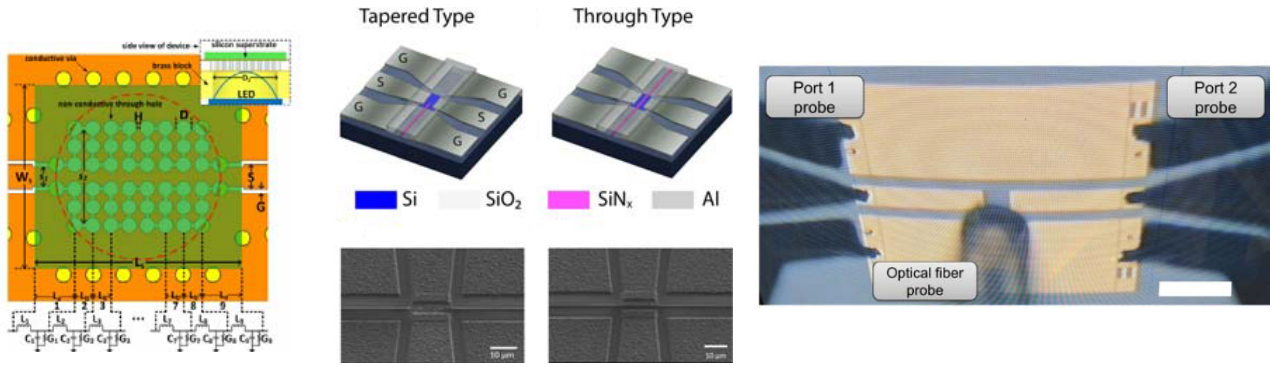

(a) (b) (c)

Figure 19. Summary of optical switches for mm-wave applications. (a) [144] © 2019 John Wiley and Sons. (b) Adapted from [145], licensed under CC BY 4.0, http://creativecommons.org/licenses/by/4.0/. (c) Adapted from [146] © 2019 John Wiley and Sons.

a series of additional fabrication steps in order to enable a smaller, less lossy PS. However, switches placed close to the feed exhibited undesirable losses. This further underscores the point that these optical switches work best when the switching mechanism is isolated further away from the dominant field sources, whether feeding or radiative in nature.

Though only a very limited number of articles have discussed the application of optically reconfigured antennas specifically for the 5G or mm-wave spectrum, some promising work has focused on designing the required switches. For PCB-type designs, work in [144] demonstrated a novel, self-contained, LED-illuminated grounded co-planar waveguide switch for mm-wave applications (Figure 19(a)). By operating the LED in a low-power 200 mW mode, the switch achieved an insertion loss of less than 2.9 dB and isolation of greater than 15 dB across the frequencies ranging from 12–30 GHz. Recent work has also focused on the design of chip-level optically controlled switches that may be fabricated using CMOS technology. In [145], the researchers demonstrated two photonic-integrated switches that steer light through CPW elements using a silicon nitride waveguide. These switches are shown in Figure 19(b). The advantage of the waveguide system removes the need to carefully arrange optical fibers as was the case for many of the other designs discussed earlier. This design is able to achieve isolation greater than 15 dB at 5 GHz and 20 GHz using a maximum optical power of 1.5 mW. However, the insertion loss ranges from 20 to 40 dB across these bands, suggesting that this type of integration would be quite lossy. It remains to be seen though, how this would compare with similarly scaled antennas, since efficiencies will already be low. The related concept of a CPW switch in [146] also reported an isolation of around 15 dB up to about 40 GHz and an average insertion loss of 25 dB using an optical power of 40 mW (Figure 19(c)). Given the similar reported insertion loss, it is likely that this loss is a factor of the CMOS-compatible fabrication technology that is used.

In summary, there have been a number of different works focused on developing optically controlled antennas and other electromagnetic devices. The main challenges are primarily centered around interfacing the custom semiconductor switch with a light source. As such, the development of a plug-and-play switch component with specified working parameters would be key to fully enabling this technology. Laser light sources are effective but tend to be more costly if they are not already included as part of a photonic down conversion or other system. On the other hand, laser diodes offer an inexpensive solution with a smaller footprint, while LED's offer a yet simpler integration method. Additionally, future work is expected to also focus on investigating the performance of other off-the-shelf solutions at higher frequency bands, such as combined phototransistor and diode integrations as discussed above. Consequently, if these challenges are met, the various benefits of optical control such as electromagnetic isolation, absence of a bias network, and fast switching speeds will be within reach for deployment in future telecommunications systems.

5. RECONFIGURABLE FREQUENCY SELECTIVE SURFACES AND METASURFACES

5.1. Space Applications

Reconfigurable metamaterial reflectarrays were introduced in the mid-2000s and are still common to this day [147]. They have been implemented in a large variety of forms for many different applications, with one of the most common being satellite communication. One notable design focuses on multispot coverage in the Ka-band [148]. This example works by producing four adjacent beams per waveguide feed. First, the feed position is calculated so that two adjacent beams can be produced at different frequencies. The other two beams are of an orthogonal polarization and are generated as the array has a different phase shift for each polarization. The unit cell itself is made of stacked parallel dipoles. This design is useful because it can potentially reduce the number of antennas and feeds required for multispot coverage in satellite communications. This work was later built upon by the same authors [149–151]. They improved the antenna to allow for circularly polarized reflected beams by applying a variable rotation technique to the unit cells at each frequency (Figure 20 below).

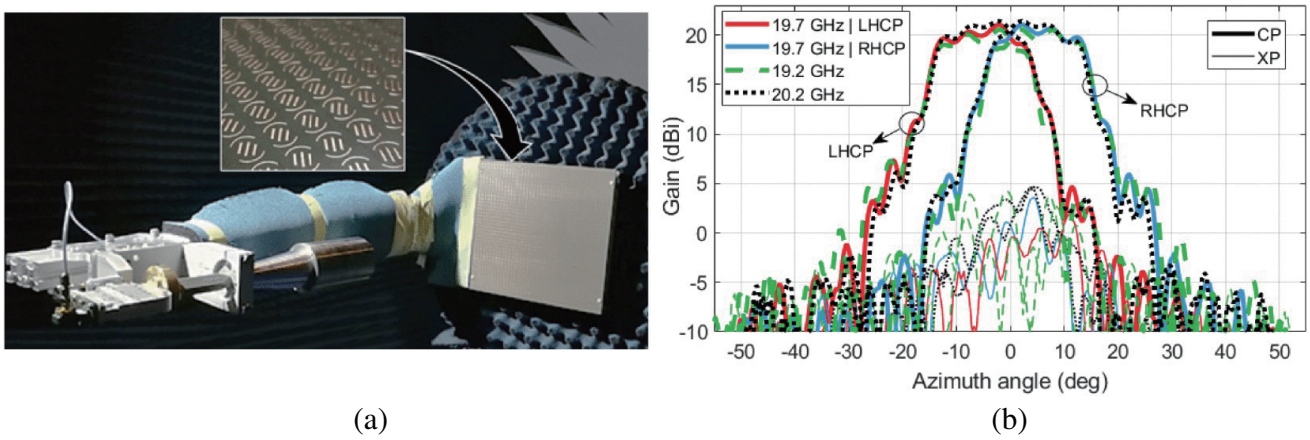

Figure 20. (a) Dual-band circularly polarized metamaterial reflectarray. (b) Resulting dual LHCP and RHCP measured beams. © 2020 IEEE. Reprinted, with permission, from [151].

In addition to multispot performance, beam steering has also been studied. One example demonstrates usefulness in Ku-band satellites as it provides a beam scanning over the frequency range of 11.5 to 15 GHz [152]. This design uses a multilayer unit cell with a 1-bit reflection phase which is changed by varying voltage in PIN diodes. This design uses an offset feed and can twist a linearly polarized wave to perform beam steering. It can also produce a circularly polarized (CP) beam, but it requires a circularly polarized feed. To take advantage of the reconfigurable nature, the researchers implemented a control code and control system to make it easy to set the direction of the beam. Another notable work performs a similar function but in the context of radar cross section (RCS) reduction [153]. A unit cell with a mushroom type structure is implemented, and its reflection phase can be varied using capacitive loading. It utilizes thermistors, varactors, and two different biasing networks. All these elements together allow this antenna to reduce RCS in the specular direction and control the placement of RCS peaks and nulls.

Many of the previously mentioned metamaterial arrays have implemented CP beams in some form. CP beams have many benefits in satellite communication such as reducing polarization mismatch, etc. However, many designs are limited by the fact that their feed source must be CP for the reflected wave to also be CP. Older designs have achieved this effect, but they were severely limited by bandwidth [154, 155]. Two more recent works have overcome this limitation through different techniques. The first uses a unit cell with an open loop and Jerusalem cross shape [156]. It has a 1-dB gain bandwidth of 12.5% and a 3-dB axial ratio bandwidth of 50%. The second employs non-resonant rectangular shaped capacitive patches which have thin dielectrics sandwiched between them [157]. Each unit cell causes a

difference in reflection phase of 90 degrees between the vertical and horizontal components. This design can operate in the X-band from 8–12 GHz.

Other designs have used foldable and mechanically configurable arrays to allow for a smaller footprint. One example uses a single panel separated into sections by a series of compliant and surrogate Lamnina Emergent Torsional joints [158]. The array can then be folded into different configurations in order to achieve different beam modes. This technology could be useful in CubeSat applications, because it requires no assembly. Another mechanically reconfigurable array uses a wideband polarization rotating metasurface and a circular waveguide [159]. It also contains a polarization grid, which means the distance between the array surface and the feed can be reduced.

One way to find potential avenues for future innovation in reconfigurable reflectarrays is to examine the current state of the art in passive arrays. Principles developed for passive structures can often be applied to reconfigurable ones. For example, a surface can be designed to be reflective in one band and transparent in another [160].

5.2. Next Generation Terrestrial

Metamaterials are used not only for space satellites but also for 5G and other terrestrial communication applications. Reconfigurable intelligent surfaces (RIS) are an emerging technology and can provide useful innovations. For clarity, RIS has other names, such as smart radio environment (SRE), intelligent radio environment (IRE), and "Wireless 2.0" [161, 162]. The main idea is to turn the environment itself into one of the parameters that can be optimized. To do this, an RIS requires sensing components to determine communication channel parameters as well as interfacing components such as a microcontroller. These surfaces can serve as useful platforms for spatial modulation and spatial modulation schemes. RFocus from MIT is a notable example [163].

One of the uses for RIS systems is related to indoor communications. An RIS can be used for electromagnetically secure buildings [164]. In many cases, shielding and jamming are not practical solutions for preventing communications. For this design, a dual-polarized, dual layer frequency selective surface has unit cells with 110 degrees of phase range composed of varactor diodes. The phase response can by dynamically reconfigured to increase the bit error rate of unwanted signals and render them unreadable. The reconfigurable nature also means that the RIS can be turned on and off with ease when communications is required or needs to be blocked. Another RIS example enables spectrum sharing in indoor environments [165] (Figure 21). It again utilizes varactors and can allow multiple wireless users to access the same spectrum band without interfering with each other or modifying their devices. Signals from RIS can be spatially modulated and projected to arbitrary regions without interfering with other regions.

Metasurfaces for 5G applications are not limited to research lab settings. There are examples of this technology being explored in industry. NTT Docomo's smart glass is a notable example as it constitutes

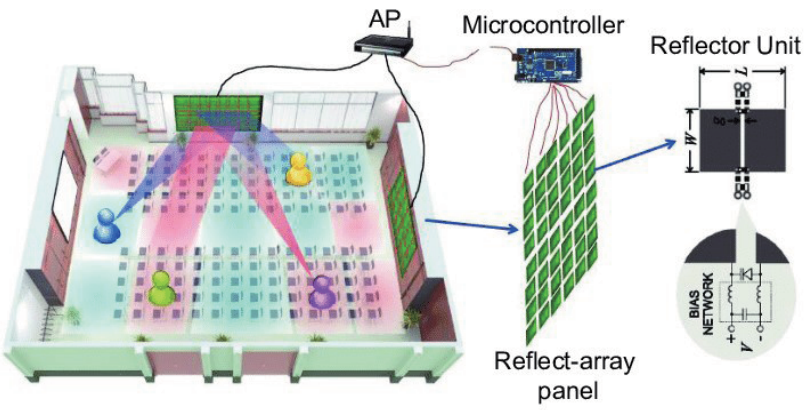

Figure 21. RIS which enables spectrum sharing indoors. © 2016 IEEE. Reprinted, with permission, from [165].

a transparent dynamic metasurface which operates with 5G radio signals at 28 GHz [166]. It can be used on billboards and windows to allow radio waves to pass through without obstruction. Another company exploring this technology is Pivotal Commware [167, 168]. They are developing Holographic Beam Forming (HBF), which is similar to a previously mentioned work, that allows wireless service providers to repeatedly reuse the same spectrum band at the same time in a certain spatial area. HBF can be much less expensive than alternative techniques such as MIMO and phased arrays because of its simpler construction.

Some next-gen communication arrays are not reconfigurable but still offer interesting innovations and could be made reconfigurable in the future. One of them is meant for use on UAVs and has a small footprint [169]. However, the beam can only be projected directly downwards. Another example of RIS can interact with polarization in novel ways [170]. Its unit cell resembles a cylinder with a cuboid cut out of it. Certain orientations of the unit cell are polarization invariant. When the orientation is changed, efficient polarization conversion can be achieved. This design can produce a fixed beam in any direction, and motors could be added to allow for dynamic beam steering. One last example is a filtering reflectarray [171]. It incorporates a coplanar band-stop filter circuit in the ground plane as well as a two-layer band-notched absorber. Therefore, it can act as a bandpass filter, a property not usually seen in reflectarrays.

While metamaterial antenna arrays are frequently used for communications, other applications have also been studied. Several works have discussed the integration of metasurfaces and solar cells [172–174]. This can be used in CubeSATs. In addition, some metasurfaces have also been used for remote sensing [175].

6. CONCLUSION AND FUTURE OF RECONFIGURABILITY

This review outlined a detailed account of several techniques for designing reconfigurable antenna systems. Throughout the manuscript, special attention has been devoted to the latest trends in this field of study. We also provide some insights into next generation reconfigurable antenna systems.

Mechanically reconfigurable systems, although relatively slow in response time, are the oldest category of techniques used for developing reconfigurable antennas. It has been shown that these methods have the potential to alleviate the need for complex biasing systems, have high power handling capabilities and offer robust solutions in meeting future 5G and 6G communication requirements. The use of techniques such as origami, fluidics, and flexible materials offers a variety of approaches to mechanically driven reconfiguration. Furthermore, mechanical methods can be combined with novel electrical technologies in order to create other types of reconfigurable antennas. Examples of these newer designs include mechanically reconfigurable metamaterial-enabled high power antenna systems and mechanically rotating shutters equipped high-gain slotted waveguides. These works have paved the way forward for further exploration of reconfigurable systems with a hybridization of both mechanical and electrical elements.

The electrical techniques for reconfigurability primarily rely on the implementation of effective switching mechanisms. This can be accomplished by traditional electronic switches such as PIN diodes, varactor diodes, FET and CMOS switches or by invoking hybrid electroomechanical MEMS technologies. PCMs offer another approach for achieving reconfigurability. A plethora of texts refer to VO_2 and Chalcogenides as excellent choices for PCMs, and investigate effects of temperature on their electrical properties. Other works discuss reconfiguration through the alteration of constituent material properties, with ferroelectrics, liquid crystals, and smart materials being some of the more prominent methods. Lastly, several authors consider resistive memory technology such as memristors and atomristors as strong candidates for future antenna applications due to several unique properties, especially their potentially low power requirements.

In the optical regime, electrical switches are replaced by photoconductive switches to attain reconfiguration. In this work, several configurations for integration of photoconductive switches within devices have been explained. Moreover, the comparative source power requirements for most of those schemes have been enumerated. In addition to standalone laser light sources and laser diodes, the possibilities of having LEDs as sources for optically reconfigurable antennas and their potential impact in future systems have also been explored.

This work concludes with the use of artificially engineered materials, metasurfaces and frequency selective surfaces in the context of reconfigurable antennas. This is a newer field of study, spanning across only a few decades. Contextually, this review focuses on satellite and terrestrial applications. Within this framework the advantages of using CP and multispot beams for satellite applications have been detailed. For the next generation terrestrial communications, new and emergent technologies such as reconfigurable intelligent surfaces have been cited. In addition, the authors also believe that these artificial materials can be efficiently used for developing reconfigurable systems catering to other aerial applications such as UAVs and drones.

In conclusion, it is expected that reconfigurable antennas will continue to play a pivotal role in meeting the continuously increasing demands of future communication systems. While numerous reconfiguration methods have been consistently evolving for many decades, others have only emerged in the recent past. The amount of published research related to this topic is vast, and the field has been growing since the turn of the millennium. It is expected that the prominence of reconfigurable antenna systems will increase further in the coming decades.

ACKNOWLEDGMENT

D. H. Werner gratefully acknowledges support from the John L. and Genevieve H. McCain endowment, The Pennsylvania State University.

REFERENCES

1. Lyke, J. C., C. G. Christodoulou, G. A. Vera, and A. H. Edwards, "An introduction to reconfigurable systems," *Proceedings of the IEEE*, Vol. 103, No. 3, 291–317, Mar. 2015, doi: 10.1109/JPROC.2015.2397832.
2. Oliveri, G., D. H. Werner, and A. Massa, "Reconfigurable electromagnetics through metamaterials — A review," *Proceedings of the IEEE*, Vol. 103, No. 7, 1034–1056, Jul. 2015, doi: 10.1109/JPROC.2015.2394292.
3. Motovilova, E. and S. Y. Huang, "A review on reconfigurable liquid dielectric antennas," *Materials*, Vol. 13, 1863, 2020.
4. Bernhard, J. T., "Reconfigurable antennas," *Synthesis Lectures on Antennas*, Vol. 2, No. 1, 1–66, Jan. 2007, doi: 10.2200/S00067ED1V01Y200707ANT004.
5. Christodoulou, C. G., Y. Tawk, S. A. Lane, and S. R. Erwin, "Reconfigurable antennas for wireless and space applications," *Proceedings of the IEEE*, Vol. 100, No. 7, 2250–2261, Jul. 2012, doi: 10.1109/JPROC.2012.2188249.
6. Ojaroudi Parchin, N., H. Jahanbakhsh Basherlou, Y. I. A. Al-Yasir, A. M. Abdulkhaleq, and R. A. Abd-Alhameed, "Reconfigurable antennas: Switching techniques — A survey," *Electronics*, Vol. 9, No. 2, 336, Feb. 2020, doi: 10.3390/electronics9020336.
7. Haupt, R. L. and M. Lanagan, "Reconfigurable antennas," *IEEE Antennas and Propagation Magazine*, Vol. 55, No. 1, 49–61, Feb. 2013, doi: 10.1109/MAP.2013.6474484.
8. Joodaki, H., H. Valiee, and M. Bayat, "Reconfigurable dual frequency microstrip MIMO patch antenna using RF MEMS switches for WLAN application," *2013 25th Chinese Control and Decision Conference (CCDC)*, 3254–3258, Guiyang, China, May 2013, doi: 10.1109/CCDC.2013.6561508.
9. Soltani, S., P. Lotfi, and R. D. Murch, "A port and frequency reconfigurable MIMO slot antenna for WLAN applications," *IEEE Transactions on Antennas and Propagation*, Vol. 64, No. 4, 1209–1217, Apr. 2016, doi: 10.1109/TAP.2016.2522470.
10. Yuan, X., et al., "A parasitic layer-based reconfigurable antenna design by multi-objective optimization," *IEEE Transactions on Antennas and Propagation*, Vol. 60, No. 6, 2690–2701, Jun. 2012, doi: 10.1109/TAP.2012.2194663.

11. Abdulraheem, Y. I., et al., "Design of frequency reconfigurable multiband compact antenna using two PIN diodes for WLAN/WiMAX applications," *IET Microwaves, Antennas and Propagation*, Vol. 11, No. 8, 1098–1105, Jun. 2017, doi: 10.1049/iet-map.2016.0814.
12. Panagamuwa, C. J., A. Chauraya, and J. C. Vardaxoglou, "Frequency and beam reconfigurable antenna using photoconducting switches," *IEEE Transactions on Antennas and Propagation*, Vol. 54, No. 2, 449–454, Feb. 2006, doi: 10.1109/TAP.2005.863393.
13. Bruce, E. and A. C. Beck, "Experiments with directivity steering for fading reduction," *Proceedings of the Institute of Radio Engineers*, Vol. 23, No. 4, 357–371, Apr. 1935, doi: 10.1109/JRPROC.1935.227992.
14. Zhu, H. L., X. H. Liu, S. W. Cheung, and T. I. Yuk, "Frequency-reconfigurable antenna using metasurface," *IEEE Transactions on Antennas and Propagation*, Vol. 62, No. 1, 80–85, Jan. 2014, doi: 10.1109/TAP.2013.2288112.
15. Ma, W., G. Wang, B.-F. Zong, Y. Zhuang, and X. Zhang, "Mechanically reconfigurable antenna based on novel metasurface for frequency tuning-range improvement," *2016 IEEE International Conference on Microwave and Millimeter Wave Technology (ICMMT)*, 629–631, 2016, doi: 10.1109/ICMMT.2016.7762390.
16. Zhu, H. L., S. W. Cheung, and T. I. Yuk, "Mechanically pattern reconfigurable antenna using metasurface," *IET Microwaves, Antennas and Propagation*, Vol. 9, No. 12, 1331–1336, 2015.
17. Filgueiras, H. R. D., I. F. da Costa, S. A. Cerqueira, R. A. Santos, and J. R. Kelly, "Mechanically reconfigurable slotted-waveguide antenna array for 5G networks," *2017 SBMO/IEEE MTT-S International Microwave and Optoelectronics Conference (IMOC)*, 1–5, 2017, doi: 10.1109/IMOC.2017.8121105.
18. Ma, X. and K. Li, "A low-profile broadband high-gain mechanically pattern reconfigurable antenna," *2020 Cross Strait Radio Science & Wireless Technology Conference (CSRSWTC)*, 1–3, 2020, doi: 10.1109/CSRSWTC50769.2020.9372532.
19. Lin, Y., W. Chen, C. Chen, C. Liao, N. Chuang, and H. Chen, "High-gain MIMO dipole antennas with mechanical steerable main beam for 5G small cell," *IEEE Antennas and Wireless Propagation Letters*, Vol. 18, No. 7, 1317–1321, Jul. 2019, doi: 10.1109/LAWP.2019.2914673.
20. Lotfi, P., M. Azarmanesh, and S. Soltani, "Rotatable dual band-notched UWB/triple-band WLAN reconfigurable antenna," *IEEE Antennas and Wireless Propagation Letters*, Vol. 12, 104–107, 2013, doi: 10.1109/LAWP.2013.2242842.
21. Zhu, H. L., S. W. Cheung, X. H. Liu, and T. I. Yuk, "Design of polarization reconfigurable antenna using metasurface," *IEEE Transactions on Antennas and Propagation*, Vol. 62, No. 6, 2891–2898, Jun. 2014, doi: 10.1109/TAP.2014.2310209.
22. McMichael, T., "A mechanically reconfigurable patch antenna with polarization diversity," *IEEE Antennas and Wireless Propagation Letters*, Vol. 17, No. 7, 1186–1189, Jul. 2018, doi: 10.1109/LAWP.2018.2837902.
23. Yao, S. and S. V. Georgakopoulos, "Origami segmented helical antenna with switchable sense of polarization," *IEEE Access*, Vol. 6, 4528–4536, 2018, doi: 10.1109/ACCESS.2017.2787724.
24. Liu, X., S. Yao, B. S. Cook, M. M. Tentzeris, and S. V. Georgakopoulos, "An origami reconfigurable axial-mode bifilar helical antenna," *IEEE Transactions on Antennas and Propagation*, Vol. 63, No. 12, 5897–5903, Dec. 2015, doi: 10.1109/TAP.2015.2481922.
25. Shah, S. I. H., M. M. Tentzeris, and S. Lim, "Low-cost circularly polarized origami antenna," *IEEE Antennas and Wireless Propagation Letters*, Vol. 16, 2026–2029, 2017, doi: 10.1109/LAWP.2017.2694138.
26. Shah, S. I. H., D. Lee, M. M. Tentzeris, and S. Lim, "A novel high-gain tetrahedron origami," *IEEE Antennas and Wireless Propagation Letters*, Vol. 16, 848–851, 2017, doi: 10.1109/LAWP.2016.2609898.
27. Hu, J., S. Lin, and F. Dai, "Pattern reconfigurable antenna based on morphing bistable composite laminates," *IEEE Transactions on Antennas and Propagation*, Vol. 65, No. 5, 2196–2207, May 2017, doi: 10.1109/TAP.2017.2677258.

28. Campbell, S. D., et al., "Extending power-handling of high-power metamaterial phase-shifters using three-dimensional counter-rotated end-loaded dipoles," *2017 IEEE International Symposium on Antennas and Propagation & USNC/URSI National Radio Science Meeting*, 91–92, 2017, doi: 10.1109/APUSNCURSINRSM.2017.8072088.
29. Campbell, S. D., G. Makertich-Sengerdy, J. D. Binion, R. J. Chaky, R. P. Jenkins, R. J. Beneck, C. A. Mussman, E. B. Whiting, P. L. Werner, D. H. Werner, S. Parrish, D. Law, J. Pompeii, and S. Griffiths, "Metamaterial-enabled reflectarray antennas for high-power microwave applications," *2020 IEEE International Symposium on Antennas & Propagation — (APSURSI)*, Montreal, QC, Canada, Jul. 5–10, 2020.
30. Jouade, A., M. Himdi, A. Chauloux, and F. Colombel, "Mechanically pattern-reconfigurable bended horn antenna for high-power applications," *IEEE Antennas and Wireless Propagation Letters*, Vol. 16, 457–460, 2017, doi: 10.1109/LAWP.2016.2583203.
31. Hua, C. and Z. Shen, "Shunt-excited sea-water monopole antenna of high efficiency," *IEEE Transactions on Antennas and Propagation*, Vol. 63, No. 11, 5185–5190, Nov. 2015, doi: 10.1109/TAP.2015.2477418.
32. Xing, L., Y. Huang, S. S. Alja'afreh, and S. J. Boyes, "A monopole water antenna," *2012 Loughborough Antennas & Propagation Conference (LAPC)*, 1–4, 2012, doi: 10.1109/LAPC.2012.6402985.
33. Huff, G. H., D. L. Rolando, P. Walters, and J. McDonald, "A frequency reconfigurable dielectric resonator antenna using colloidal dispersions," *IEEE Antennas and Wireless Propagation Letters*, Vol. 9, 288–290, 2010, doi: 10.1109/LAWP.2010.2046613.
34. Ren, J. and J. Y. Yin, "Cylindrical-water-resonator-based ultra-broadband microwave absorber," *Opt. Mater. Express*, Vol. 8, 2060–2071, 2018.
35. Kasiriga, T. S., Y. N. Erlas, and M. Bayindir, "Microfluidics for reconfigurable electromagnetic metamaterials," *Appl. Phys. Lett.*, Vol. 95, Art. ID 214102, 2009.
36. Rodrigo, D., L. Jofre, and B. A. Cetiner, "Circular beam-steering reconfigurable antenna with liquid metal parasitics," *IEEE Transactions on Antennas and Propagation*, Vol. 60, No. 4, 1796–1802, Apr. 2012, doi: 10.1109/TAP.2012.2186235.
37. Su, W., S. A. Nauroze, B. Ryan, and M. M. Tentzeris, "Novel 3D printed liquid-metal-alloy microfluidics-based Zigzag and helical antennas for origami reconfigurable antenna "Trees"," *2017 IEEE MTT-S International Microwave Symposium (IMS)*, 1579–1582, 2017, doi: 10.1109/MWSYM.2017.8058933.
38. Jiang, W., L. Zhou, F. Wang, J. Shi, and Y. Liang, "Structural design and realization of a mechanical reconfigurable antenna," *2018 International Conference on Electronics Technology (ICET)*, 349–353, 2018, doi: 10.1109/ELTECH.2018.8401401.
39. Moghadas, H., M. Zandvakili, D. Sameoto, and P. Mousavi, "Beam-reconfigurable aperture antenna by stretching or reshaping of a flexible surface," *IEEE Antennas and Wireless Propagation Letters*, Vol. 16, 1337–1340, 2017, doi: 10.1109/LAWP.2016.2633964.
40. Chaudhari, S., S. Alharbi, C. Zou, H. Shah, R. L. Harne, and A. Kiourti, "A new class of reconfigurable origami antennas based on E-textile embroidery," *2018 IEEE International Symposium on Antennas and Propagation & USNC/URSI National Radio Science Meeting*, 183–184, 2018, doi: 10.1109/APUSNCURSINRSM.2018.8608203.
41. Kowalewski, J., J. Mayer, T. Mahler, and T. Zwick, "A compact pattern reconfigurable antenna utilizing multiple monopoles," *2016 International Workshop on Antenna Technology (iWAT)*, 1–4, Cocoa Beach, FL, USA, Feb. 2016, doi: 10.1109/IWAT.2016.7434783.
42. Rajagopalan, H., J. M. Kovitz, and Y. Rahmat-Samii, "MEMS reconfigurable optimized E-shaped patch antenna design for cognitive radio," *IEEE Transactions on Antennas and Propagation*, Vol. 62, No. 3, 1056–1064, Mar. 2014, doi: 10.1109/TAP.2013.2292531.
43. Yang, X., J. Lin, G. Chen, and F. Kong, "Frequency reconfigurable antenna for wireless communications using GaAs FET switch," *IEEE Antennas and Wireless Propagation Letters*, Vol. 14, 807–810, Dec. 2015, doi: 10.1109/LAWP.2014.2380436.

44. Bhattacharya, A. and R. Jyoti, "Frequency reconfigurable patch antenna using PIN diode at X-band," *2015 IEEE 2nd International Conference on Recent Trends in Information Systems (ReTIS)*, 81–86, Kolkata, India, Jul. 2015, doi: 10.1109/ReTIS.2015.7232857.
45. Ali, M., A. T. M. Sayem, and V. K. Kunda, "A reconfigurable stacked microstrip patch antenna for satellite and terrestrial links," *IEEE Trans. Veh. Technol.*, Vol. 56, No. 2, 426–435, Mar. 2007, doi: 10.1109/TVT.2007.891412.
46. Lotfi, P., S. Soltani, and R. D. Murch, "Printed endfire beam-steerable pixel antenna," *IEEE Transactions on Antennas and Propagation*, Vol. 65, No. 8, 3913–3923, Aug. 2017, doi: 10.1109/TAP.2017.2716399.
47. George, R., S. Kumar, S. A. Gangal, and M. Joshi, "Frequency reconfigurable pixel antenna with PIN diodes," *Progress In Electromagnetics Research Letters*, Vol. 86, 59–65, 2019.
48. Sulakshana, C. and L. Anjaneyulu, "A compact reconfigurable antenna with frequency, polarization and pattern diversity," *Journal of Electromagnetic Waves and Applications*, Vol. 29, No. 15, 1953–1964, Oct. 2015, doi: 10.1080/09205071.2015.1068229.
49. Wang, M., et al., "Design and measurement of a Ku-band pattern-reconfigurable array antenna using 16 O-slot patch elements with p-i-n diodes," *IEEE Antennas and Wireless Propagation Letters*, Vol. 19, No. 12, 2373–2377, Dec. 2020, doi: 10.1109/LAWP.2020.3033355.
50. Yashchyshyn, Y., et al., "28 GHz switched-beam antenna based on S-PIN diodes for 5G mobile communications," *IEEE Antennas and Wireless Propagation Letters*, Vol. 17, No. 2, 225–228, Feb. 2018, doi: 10.1109/LAWP.2017.2781262.
51. Xiao, Y., B. Xi, M. Xiang, F. Yang, and Z. Chen, "1-bit wideband reconfigurable transmitarray unit cell based on PIN diodes in Ku-band," *IEEE Antennas and Wireless Propagation Letters*, 1–1, 2021, doi: 10.1109/LAWP.2021.3100494.
52. Gregory, M. D., S. V. Martin, and D. H. Werner, "Improved electromagnetics optimization: The covariance matrix adaptation evolutionary strategy," *IEEE Antennas and Propagation Magazine*, Vol. 57, No. 3, 48–59, Jun. 2015, doi: 10.1109/MAP.2015.2437277.
53. Srivastava, S., P. Mishra, and R. K. Singh, "Design of a reconfigurable antenna with fractal geometry," *2015 IEEE UP Section Conference on Electrical Computer and Electronics (UPCON)*, 1–6, Allahabad, India, Dec. 2015, doi: 10.1109/UPCON.2015.7456687.
54. Scarborough, C. P., D. H. Werner, and D. E. Wolfe, "Compact low-profile tunable metasurface-enabled antenna with near-arbitrary polarization," *IEEE Transactions on Antennas and Propagation*, Vol. 64, No. 7, 2775–2783, Jul. 2016, doi: 10.1109/TAP.2016.2562666.
55. Scarborough, C. P., D. H. Werner, and D. E. Wolfe, "Functionalized metamaterials enable frequency and polarization agility in a miniaturized lightweight antenna package," *Advanced Electronic Materials*, Vol. 2, No. 2, Art. no. 1500295, Feb. 2016.
56. Luxey, C. and J.-M. Laheurte, "Effect of reactive loading in microstrip leaky wave antennas," *Electronics Letters*, Vol. 36, No. 15, 1259–1260, 2000, doi: 10.1049/el:20000932.
57. Ouedraogo, R. O., E. J. Rothwell, and B. J. Greetis, "A reconfigurable microstrip leaky-wave antenna with a broadly steerable beam," *IEEE Transactions on Antennas and Propagation*, Vol. 59, No. 8, 3080–3083, Aug. 2011, doi: 10.1109/TAP.2011.2158970.
58. Suntives, A. and S. V. Hum, "A fixed-frequency beam-steerable half-mode substrate integrated waveguide leaky-wave antenna," *IEEE Transactions on Antennas and Propagation*, Vol. 60, No. 5, 2540–2544, May 2012, doi: 10.1109/TAP.2012.2189726.
59. Suntives, A. and S. V. Hum, "An electronically tunable half-mode substrate integrated waveguide leaky-wave antenna," *Proceedings of the 5th European Conference on Antennas and Propagation (EUCAP)*, 3670–3674, 2011.
60. Mohsen, M. K., M. S. M. Isa, A. A. M. Isa, M. K. Abdulhameed, and M. L. Attiah, "Achieving fixed-frequency beam scanning with a microstrip leaky-wave antenna using double-gap capacitor technique," *IEEE Antennas and Wireless Propagation Letters*, Vol. 18, No. 7, 1502–1506, Jul. 2019, doi: 10.1109/LAWP.2019.2920940.
61. Maryam, S. and A. Pourziad, "A novel reconfigurable spiral-shaped monopole antenna for biomedical applications," *Progress In Electromagnetics Research Letters*, Vol. 57, 79–84, 2015.

62. Prasad, G. R., et al., "Concentric ring structured reconfigurable antenna using MEMS switches for wireless communication applications," *Wireless Personal Communications*, Vol. 120, No. 1, 587–608, Sep. 2021, doi: 10.1007/s11277-021-08480-6.
63. Xu, Y., Y. Tian, B. Zhang, J. Duan, and L. Yan, "A novel RF MEMS switch on frequency reconfigurable antenna application," *Microsystem Technologies*, Vol. 24, No. 9, 3833–3841, Sep. 2018, doi: 10.1007/s00542-018-3863-9.
64. Bray, M. G. and D. H. Werner, "Passive switching of electromagnetic devices with memristors," *Appl. Phys. Lett.*, Vol. 96, 073504/1–3, Feb. 2010, doi: 10.1063/1.3299020.
65. Gregory, M. D. and D. H. Werner, "Application of the memristor in reconfigurable electromagnetic devices," *IEEE Antennas and Propagation Magazine*, Vol. 57, No. 1, 239–248, Feb. 2015, doi: 10.1109/MAP.2015.2397153.
66. Strukov, D. B., G. S. Snider, D. R. Stewart, and R. S. Williams, "The missing memristor found," *Nature*, Vol. 453, No. 7191, 80–83, May 2008, doi: 10.1038/nature06932.
67. Werner, D. H. and M. D. Gregory, "The memristor in reconfigurable radio frequency devices," *Proceedings of the 2012 IEEE International Symposium on Antennas and Propagation*, 1–2, 2012, doi: 10.1109/APS.2012.6349274.
68. Gregory, M. D. and D. H. Werner, "Reconfigurable electromagnetics devices enabled by a non-linear dopant drift memristor," *2014 IEEE Antennas and Propagation Society International Symposium (APSURSI)*, 563–564, 2014, doi: 10.1109/APS.2014.6904612.
69. Zhao, G. and B. You, "A tunable bandpass-to-bandstop filter using memristor and varactors," *2020 IEEE MTT-S International Conference on Numerical Electromagnetic and Multiphysics Modeling and Optimization (NEMO)*, 1–4, Hangzhou, China, Dec. 2020, doi: 10.1109/NEMO49486.2020.9343581.
70. Pi, S., M. Ghadiri-Sadrabadi, J. C. Bardin, and Q. Xia, "Nanoscale memristive radiofrequency switches," *Nat. Commun.*, Vol. 6, No. 1, 7519, Nov. 2015, doi: 10.1038/ncomms8519.
71. Wu, X., R. Ge, M. Kim, D. Akinwande, and J. C. Lee, "Atomristors: Non-volatile resistance switching in 2D monolayers," *2020 Pan Pacific Microelectronics Symposium (Pan Pacific)*, 1–6, HI, USA, Feb. 2020, doi: 10.23919/PanPacific48324.2020.9059369.
72. Kim, M., et al., "Zero-static power radio-frequency switches based on MoS_2 atomristors," *Nat. Commun.*, Vol. 9, No. 1, 2524, Dec. 2018, doi: 10.1038/s41467-018-04934-x.
73. Wang, M., F. Lin, and M. Rais-Zadeh, "Need a change? Try GeTe: A reconfigurable filter using germanium telluride phase change RF switches," *IEEE Microwave*, Vol. 17, No. 12, 70–79, Dec. 2016, doi: 10.1109/MMM.2016.2608699.
74. Chau, L., J. G. Ho, X. Lan, G. Altvater, R. M. Young, N. El-Hinnawy, et al., "Optically controlled GeTe phase change switch and its applications in reconfigurable antenna arrays," *Proc. SPIE*, Vol. 9479, 947905, 2015, doi: 10.1117/12.2179852.
75. Dumas-Bouchiat, F., C. Champeaux, A. Catherinot, A. Crunteanu, and P. Blondy, "RF-microwave switches based on reversible semiconductor-metal transition of VO_2 thin films synthesized by pulsed-laser deposition," *Appl. Phys. Lett.*, Vol. 91, No. 22, 223505, Nov. 2007, doi: 10.1063/1.2815927.
76. Hillman, C., P. A. Stupar, J. B. Hacker, Z. Griffith, M. Field, and M. Rodwell, "An ultra-low loss millimeter-wave solid state switch technology based on the metal-insulator-transition of vanadium dioxide," *2014 IEEE MTT-S International Microwave Symposium (IMS2014)*, 1–4, Jun. 2014, doi: 10.1109/MWSYM.2014.6848479.
77. Field, M., C. Hillman, P. Stupar, J. Hacker, Z. Griffith, and K.-J. Lee, "Vanadium dioxide phase change switches," *Open Architecture/Open Business Model Net-Centric Systems and Defense Transformation 2015*, Vol. 9479, 947908, May 2015, doi: 10.1117/12.2179851.
78. Hillman, C., P. A. Stupar, and Z. Griffith, "VO_2 switches for millimeter and submillimeter-wave applications," *2015 IEEE Compound Semiconductor Integrated Circuit Symposium (CSICS)*, 1–4, Oct. 2015, doi: 10.1109/CSICS.2015.7314528.
79. Liu, L., L. Kang, T. S. Mayer, and D. H. Werner, "Hybrid metamaterials for electrically triggered multifunctional control," *Nature Communications*, Vol. 7, No. 13236, 1–8, 2016.

80. Vaseem, M., Z. Su, S. Yang, and A. Shamim, "Fully printed flexible and reconfigurable antenna with novel phase change VO_2 Ink based switch," *2018 International Flexible Electronics Technology Conference (IFETC)*, 1–2, Aug. 2018, doi: 10.1109/IFETC.2018.8583904.
81. Yang, S., M. Vaseem, and A. Shamim, "Fully inkjet-printed VO2-based radio-frequency switches for flexible reconfigurable components," *Advanced Materials Technologies*, Vol. 4, No. 1, 1800276, 2019, doi: 10.1002/admt.201800276.
82. Vaseem, M., S. Zhen, S. Yang, and A. Shamim, "A fully printed switch based on VO2 ink for reconfigurable RF components," *2018 48th European Microwave Conference (EuMC)*, 487–490, Sep. 2018, doi: 10.23919/EuMC.2018.8541794.
83. Chua, E. K., et al., "Low resistance, high dynamic range reconfigurable phase change switch for radio frequency applications," *Appl. Phys. Lett.*, Vol. 97, No. 18, 183506, Nov. 2010, doi: 10.1063/1.3508954.
84. Lo, H., et al., "Three-terminal probe reconfigurable phase-change material switches," *IEEE Transactions on Electron Devices*, Vol. 57, No. 1, 312–320, Jan. 2010, doi: 10.1109/TED.2009.2035533.
85. El-Hinnawy, N., et al., "A 7.3 THz cut-off frequency, inline, chalcogenide phase-change RF switch using an independent resistive heater for thermal actuation," *2013 IEEE Compound Semiconductor Integrated Circuit Symposium (CSICS)*, 1–4, Oct. 2013, doi: 10.1109/CSICS.2013.6659195.
86. El-Hinnawy, N., et al., "A four-terminal, inline, chalcogenide phase-change RF switch using an independent resistive heater for thermal actuation," *IEEE Electron Device Letters*, Vol. 34, No. 10, 1313–1315, Oct. 2013, doi: 10.1109/LED.2013.2278816.
87. El-Hinnawy, N., et al., "12.5 THz Fco GeTe inline phase-change switch technology for reconfigurable RF and switching applications," *2014 IEEE Compound Semiconductor Integrated Circuit Symposium (CSICS)*, 1–3, Oct. 2014, doi: 10.1109/CSICS.2014.6978522.
88. Shim, Y., G. Hummel, and M. Rais-Zadeh, "RF switches using phase change materials," *2013 IEEE 26th International Conference on Micro Electro Mechanical Systems (MEMS)*, 237–240, Taipei, Taiwan, Jan. 2013, doi: 10.1109/MEMSYS.2013.6474221.
89. Léon, A., et al., "In-depth caracterisation of the structural phase change of germanium telluride for RF switches," *2017 IEEE MTT-S International Microwave Workshop Series on Advanced Materials and Processes for RF and THz Applications (IMWS-AMP)*, 1–3, Sep. 2017, doi: 10.1109/IMWS-AMP.2017.8247378.
90. Moon, J.-S., H.-C. Seo, and D. Le, "Development toward high-power sub-1-ohm DC-67 GHz RF switches using phase change materials for reconfigurable RF front-end," *2014 IEEE MTT-S International Microwave Symposium (IMS 2014)*, 1–3, Jun. 2014, doi: 10.1109/MWSYM.2014.6848334.
91. Moon, J.-S., H.-C. Seo, and D. Le, "High linearity 1-Ohm RF switches with phase-change materials," *2014 IEEE 14th Topical Meeting on Silicon Monolithic Integrated Circuits in RF Systems*, 7–9, Jan. 2014, doi: 10.1109/SiRF.2014.6828512.
92. Moon, J.-S., et al., "11 THz figure-of-merit phase-change RF switches for reconfigurable wireless front-ends," *2015 IEEE MTT-S International Microwave Symposium*, 1–4, May 2015, doi: 10.1109/MWSYM.2015.7167005.
93. Léon, A., B. Reig, V. Puyal, E. Perret, P. Ferrari, and F. Podevin, "High performance and low energy consumption in phase change material RF switches," *2018 48th European Microwave Conference (EuMC)*, 491–494, Sep. 2018, doi: 10.23919/EuMC.2018.8541622.
94. Moon, J.-S., H.-C. Seo, K.-A. Son, K. Lee, D. Zehnder, and H. Tai, "5 THz figure-of-merit reliable phase-change RF switches for millimeter-wave applications," *2018 IEEE/MTT-S International Microwave Symposium — IMS*, 836–838, Jun. 2018, doi: 10.1109/MWSYM.2018.8439479.
95. Iskander, M. F., Z. Yun, Z. Zhang, R. Jensen, and S. Redd, "Design of a low-cost 2-D beam-steering antenna using ferroelectric material and CTS technology," *IEEE Transactions on Microwave Theory and Techniques*, Vol. 49, No. 5, 1000–1003, May 2001, doi: 10.1109/22.920163.

96. Lovat, G., P. Burghignoli, and S. Celozzi, "A tunable ferroelectric antenna for fixed-frequency scanning applications," *IEEE Antennas and Wireless Propagation Letters*, Vol. 5, 353–356, 2006, doi: 10.1109/LAWP.2006.880694.
97. Sazegar, M., et al., "Low-cost phased-array antenna using compact tunable phase shifters based on ferroelectric ceramics," *IEEE Transactions on Microwave Theory and Techniques*, Vol. 59, No. 5, 1265–1273, May 2011, doi: 10.1109/TMTT.2010.2103092.
98. Sazegar, M., Y. Zheng, H. Maune, X. Zhou, C. Damm, and R. Jakoby, "Compact left handed coplanar strip line phase shifter on screen printed BST," *2011 IEEE MTT-S International Microwave Symposium*, 1–4, Jun. 2011, doi: 10.1109/MWSYM.2011.5972805.
99. Aspe, B., et al., "Frequency-tunable slot-loop antenna based on KNN ferroelectric interdigitated varactors," *IEEE Antennas and Wireless Propagation Letters*, Vol. 20, No. 8, 1414–1418, Aug. 2021, doi: 10.1109/LAWP.2021.3084320.
100. Giddens, H., H. Zhang, C. Yu, and Y. Hao, "Bulk ferroelectric materials for reconfigurable antenna applications," *12th European Conference on Antennas and Propagation (EuCAP 2018)*, 316 (4 pp.)–316 (4 pp.), London, UK, 2018, doi: 10.1049/cp.2018.0675.
101. Hu, W., M. Y. Ismail, R. Cahill, J. A. Encinar, V. Fusco, H. S. Gamble, D. Linton, R. Dickie, N. Grant, and S. P. Rea, "Liquid-crystal-based reflectarray antenna with electronically switchable monopulse patterns," *Electronics Letters*, Vol. 43, No. 14, 744–745, Jul. 2007, doi: 10.1049/EL:20071098.
102. Yang, F. and J. R. Sambles, "Determination of the permittivity of nematic liquid crystals in the microwave region," *Liquid Crystals*, Vol. 30, No. 5, 599–602, May 2003, doi: 10.1080/0267829031000097466.
103. Mueller, S., et al., "Broad-band microwave characterization of liquid crystals using a temperature-controlled coaxial transmission line," *IEEE Transactions on Microwave Theory and Techniques*, Vol. 53, No. 6, 1937–1945, Jun. 2005, doi: 10.1109/TMTT.2005.848842.
104. Hu, W., et al., "Liquid crystal tunable mmWave frequency selective surface," *IEEE Microwave and Wireless Components Letters*, Vol. 17, No. 9, 667–669, Sep. 2007, doi: 10.1109/LMWC.2007.903455.
105. Bossard, J. A., et al., "Tunable frequency selective surfaces and negative-zero-positive index metamaterials based on liquid crystals," *IEEE Transactions on Antennas and Propagation*, Vol. 56, No. 5, 1308–1320, May 2008, doi: 10.1109/TAP.2008.922174.
106. Wang, X., D.-H. Kwon, D. H. Werner, I.-C. Khoo, A. V. Kildishev, and V. M. Shalaev, "Tunable optical negative-index metamaterials employing anisotropic liquid crystals," *Applied Physics Letters*, Vol. 91, 143122/1–3, Oct. 2007, doi: 10.1063/1.2795345.
107. Kwon, D.-H., D. H. Werner, I.-C. Khoo, A. V. Kildishev, and V. M. Shalaev, "Liquid crystal clad metamaterial with a tunable negative-zero-positive index of refraction," *Proceedings of the 2007 IEEE Antennas and Propagation Society International Symposium*, 2828–2831, Honolulu, Hawaii, USA, Jun. 10–15, 2007.
108. Wang, X., D.-H. Kwon, D. H. Werner, and I.-C. Khoo, "Anisotropic liquid crystals for tunable optical negative-index metamaterials," *2008 IEEE Antennas and Propagation Society International Symposium*, 1–4, 2008, doi: 10.1109/APS.2008.4619734.
109. Werner, D. H., D.-H. Kwon, I.-C. Khoo, A. V. Kildishev, and V. M. Shalaev, "Liquid crystal clad near-infrared metamaterials with tunable negative-zero-positive refractive indices," *Optics Express*, Vol. 15, No. 6, 3342–3347, Mar. 19, 2007, doi: 10.1364/OE.15.003342.
110. Liu, L. and R. J. Langley, "Liquid crystal tunable microstrip patch antenna," *Electronics Letters*, Vol. 44, No. 20, 1179–1180, Sep. 2008, doi: 10.1049/el:20081995.
111. Perez-Palomino, G., et al., "Design and demonstration of an electronically scanned reflectarray antenna at 100 GHz using multiresonant cells based on liquid crystals," *IEEE Transactions on Antennas and Propagation*, Vol. 63, No. 8, 3722–3727, Aug. 2015, doi: 10.1109/TAP.2015.2434421.
112. Gibson, J. and S. V. Georgakopoulos, "Reconfigurable antenna using shape memory polymers," *2016 IEEE International Symposium on Antennas and Propagation (APSURSI)*, 1673–1674, Jun. 2016, doi: 10.1109/APS.2016.7696543.

113. Dai, J.-W., H.-L. Peng, Y.-P. Zhang, and J.-F. Mao, "A novel tunable microstrip patch antenna using liquid crystal," *Progress In Electromagnetics Research C*, Vol. 71, 101–109, 2017.
114. Xu, G., H.-L. Peng, C. Sun, J.-G. Lu, Y. Zhang, and W.-Y. Yin, "Differential probe fed liquid crystal-based frequency tunable circular ring patch antenna," *IEEE Access*, Vol. 6, 3051–3058, 2018, doi: 10.1109/ACCESS.2017.2786870.
115. Sboui, F., J. Machac, L. Latrach, and A. Gharsallah, "Triple band tunable SIW cavity antenna with cristal liquid materials for wireless applications," *2019 IEEE 19th Mediterranean Microwave Symposium (MMS)*, 1–4, Hammamet, Tunisia, Oct. 2019, doi: 10.1109/MMS48040.2019.9157250.
116. Jiang, D., et al., "Liquid crystal-based wideband reconfigurable leaky wave X-band antenna," *IEEE Access*, Vol. 7, 127320–127326, 2019, doi: 10.1109/ACCESS.2019.2939097.
117. Hu, Z., S. Wang, Z. Shen, and W. Wu, "Broadband polarization-reconfigurable water spiral antenna of low profile," *IEEE Antennas and Wireless Propagation Letters*, Vol. 16, 1377–1380, 2017, doi: 10.1109/LAWP.2016.2636923.
118. Wang, S., L. Zhu, and W. Wu, "A novel frequency-reconfigurable patch antenna using low-loss transformer oil," *IEEE Transactions on Antennas and Propagation*, Vol. 65, No. 12, 7316–7321, Dec. 2017, doi: 10.1109/TAP.2017.2758204.
119. Singh, A., I. Goode, and C. E. Saavedra, "A multistate frequency reconfigurable monopole antenna using fluidic channels," *IEEE Antennas and Wireless Propagation Letters*, Vol. 18, No. 5, 856–860, May 2019, doi: 10.1109/LAWP.2019.2903781.
120. Chen, Z., H.-Z. Li, H. Wong, X. Zhang, and T. Yuan, "A circularly-polarized-reconfigurable patch antenna with liquid dielectric," *IEEE Open J. Antennas Propag.*, Vol. 2, 396–401, 2021, doi: 10.1109/OJAP.2021.3064996.
121. Schwering, F. K. and S.-T. Peng, "Design of dielectric grating antennas for millimeter-wave applications," *IEEE Transactions on Microwave Theory and Techniques*, Vol. 31, No. 2, 199–209, Feb. 1983, doi: 10.1109/TMTT.1983.1131458.
122. Hammad, H. F., Y. M. M. Antar, A. P. Freundorfer, and M. Sayer, "A new dielectric grating antenna at millimeter wave frequency," *IEEE Transactions on Antennas and Propagation*, Vol. 52, No. 1, 36–44, Jan. 2004, doi: 10.1109/TAP.2003.820977.
123. Ma, Z. L., K. B. Ng, C. H. Chan, and L. J. Jiang, "A novel supercell-based dielectric grating dual-beam leaky-wave antenna for 60-GHz applications," *IEEE Transactions on Antennas and Propagation*, Vol. 64, No. 12, 5521–5526, Dec. 2016, doi: 10.1109/TAP.2016.2621031.
124. Li, J., M. He, C. Wu, and C. Zhang, "Radiation-pattern-reconfigurable graphene leaky-wave antenna at terahertz band based on dielectric grating structure," *IEEE Antennas and Wireless Propagation Letters*, Vol. 16, 1771–1775, 2017, doi: 10.1109/LAWP.2017.2676121.
125. Li, J., M. He, C. Zhang, and H. Sun, "Design of reconfigurable graphene leaky-wave antenna based on dielectric grating," *2016 IEEE International Conference on Microwave and Millimeter Wave Technology (ICMMT)*, 104–106, 2016, doi: 10.1109/ICMMT.2016.7761691.
126. Hu, Z., Z. Shen, and W. Wu, "Reconfigurable leaky-wave antenna based on periodic water grating," *IEEE Antennas and Wireless Propagation Letters*, Vol. 13, 134–137, 2014, doi: 10.1109/LAWP.2014.2298245.
127. Lee, C., P. Mak, and A. De Fonzo, "Optical control of millimeter-wave propagation in dielectric waveguides," *IEEE Journal of Quantum Electronics*, Vol. 16, No. 3, 277–288, Mar. 1980, doi: 10.1109/JQE.1980.1070468.
128. Pendharker, S., R. K. Shevgaonkar, and A. N. Chandorkar, "Optically controlled frequency switching band stop filter," *2012 IEEE Asia-Pacific Conference on Antennas and Propagation*, 151–152, Aug. 2012, doi: 10.1109/APCAP.2012.6333201.
129. Ojaroudi Parchin, N., H. Jahanbakhsh Basherlou, Y. I. A. Al-Yasir, A. M. Abdulkhaleq, and R. A. Abd-Alhameed, "Reconfigurable antennas: Switching techniques — A survey," *Electronics*, Vol. 9, No. 2, 336, Feb. 2020.
130. Tawk, Y., A. R. Albrecht, S. Hemmady, G. Balakrishnan, and C. G. Christodoulou, "Optically pumped frequency reconfigurable antenna design," *IEEE Antennas and Wireless Propagation Letters*, Vol. 9, 280–283, 2010, doi: 10.1109/LAWP.2010.2047373.

131. Tawk, Y., J. Costantine, S. Hemmady, G. Balakrishnan, K. Avery, and C. G. Christodoulou, "Demonstration of a cognitive radio front end using an optically pumped reconfigurable antenna system (OPRAS)," *IEEE Transactions on Antennas and Propagation*, Vol. 60, No. 2, 1075–1083, Feb. 2012, doi: 10.1109/TAP.2011.2173139.
132. Zhao, D., Y. Han, F. Liang, Q. Zhang, and B.-Z. Wang, "Low-power optically controlled patch antenna of reconfigurable beams," *International Journal of Antennas and Propagation*, Aug. 28, 2014, https://www.hindawi.com/journals/ijap/2014/978258/ (accessed Jan. 22, 2021).
133. Pendharker, S., R. K. Shevgaonkar, and A. N. Chandorkar, "Optically controlled frequency-reconfigurable microstrip antenna with low photoconductivity," *IEEE Antennas and Wireless Propagation Letters*, Vol. 13, 99–102, 2014, doi: 10.1109/LAWP.2013.2296621.
134. Silva, L. G., A. A. C. Alves, and A. C. Sodré, "Optically controlled reconfigurable filtenna," *International Journal of Antennas and Propagation*, Vol. 2016, Article ID 7161070, 9 pages, Mar. 2016, doi: 10.1155/2016/7161070.
135. Sodré, A. C., I. Feliciano da Costa, L. T. Manera, and J. A. Diniz, "Optically controlled reconfigurable antenna array based on E-shaped elements," *International Journal of Antennas and Propagation*, Apr. 27, 2014, https://www.hindawi.com/journals/ijap/2014/750208/ (accessed Jan. 18, 2021).
136. Shepeleva, E., M. Makurin, A. Vilenskiy, and S. Chernyshev, "MM-wave patch antenna with embedded photoconductive elements for 1-bit phase shifting," *2019 PhotonIcs & Electromagnetics Research Symposium — Spring (PIERS-Spring)*, 578–581, Rome, Italy, Jun. 17–20, 2019.
137. Zhao, D., Y. Han, Q. Zhang, and B.-Z. Wang, "Experimental study of silicon-based microwave switches optically driven by LEDs," *Microwave and Optical Technology Letters*, Vol. 57, No. 12, 2768–2774, 2015, doi: https://doi.org/10.1002/mop.29435.
138. Patron, D., A. S. Daryoush, and K. R. Dandekar, "Optical control of reconfigurable antennas and application to a novel pattern-reconfigurable planar design," *Journal of Lightwave Technology*, Vol. 32, No. 20, 3394–3402, Oct. 2014, doi: 10.1109/JLT.2014.2321406.
139. Da Costa, I. F., C. S. Arismar, E. Reis, D. H. Spadoti, and J. R. M. Neto, "Optically controlled reconfigurable antenna array based on a slotted circular waveguide," *2015 9th European Conference on Antennas and Propagation (EuCAP)*, 1–4, Apr. 2015.
140. Da Costa, I. F., A. C. S, D. H. Spadoti, L. G. da Silva, J. A. J. Ribeiro, and S. E. Barbin, "Optically controlled reconfigurable antenna array for mm-Wave applications," *IEEE Antennas and Wireless Propagation Letters*, Vol. 16, 2142–2145, 2017, doi: 10.1109/LAWP.2017.2700284.
141. Da Costa, I. F., et al., "Photonics-assisted wireless link based on mm-Wave reconfigurable antennas," *IET Microwaves, Antennas & Propagation*, Vol. 11, No. 14, 2071–2076, 2017, doi: 10.1049/iet-map.2017.0178.
142. Da Costa, I. F., et al., "Optically controlled reconfigurable antenna for 5G future broadband cellular communication networks," *Journal of Microwaves, Optoelectronics and Electromagnetic Applications*, Vol. 16, No. 1, 208–217, Mar. 2017, doi: 10.1590/2179-10742017v16i1883.
143. Collett, M. A., C. D. Gamlath, and M. Cryan, "An optically tunable cavity-backed slot antenna," *IEEE Transactions on Antennas and Propagation*, Vol. 65, No. 11, 6134–6139, Nov. 2017, doi: 10.1109/TAP.2017.2755726.
144. Zhang, Y., A. W. Pang, and M. J. Cryan, "Optically controlled millimetre-wave switch with stepped-impedance lines," *IET Microwaves, Antennas & Propagation*, Vol. 13, No. 10, 1737–1741, 2019, doi: https://doi.org/10.1049/iet-map.2018.6191.
145. Fang, C.-Y., H.-H. Lin, M. Alouini, Y. Fainman, and A. El Amili, "Microwave signal switching on a silicon photonic chip," *Scientific Reports*, Vol. 9, No. 1, Art. no. 1, Aug. 2019, doi: 10.1038/s41598-019-47683-7.
146. Drisko, J. A., A. D. Feldman, F. Quinlan, J. C. Booth, N. D. Orloff, and C. J. Long, "Impedance tuning with photoconductors to 40 GHz," *IET Optoelectronics*, Vol. 13, No. 4, 177–182, 2019, doi: https://doi.org/10.1049/iet-opt.2018.5102.

147. Hum, S. V., M. Okoniewski, and R. J. Davies, "Modeling and design of electronically tunable reflectarrays," *IEEE Transactions on Antennas and Propagation*, Vol. 55, No. 8, 2200–2210, Aug. 2007, doi: 10.1109/TAP.2007.902002.
148. Martinez-De-Rioja, D., E. Martinez-De-Rioja, J. A. Encinar, R. Florencio, and G. Toso, "Reflectarray to generate four adjacent beams per feed for multispot satellite antennas," *IEEE Transactions on Antennas and Propagation*, Vol. 67, No. 2, 1265–1269, Feb. 2019, doi: 10.1109/TAP.2018.2880117.
149. Martinez-de-Rioja, D., R. Florencio, J. A. Encinar, E. Carrasco, and R. R. Boix, "Dual-frequency reflectarray cell to provide opposite phase shift in dual circular polarization with application in multibeam satellite antennas," *IEEE Antennas and Wireless Propagation Letters*, Vol. 18, No. 8, 1591–1595, Aug. 2019, doi: 10.1109/LAWP.2019.2924354.
150. Martinez-de-Rioja, E., et al., "Advanced multibeam antenna configurations based on reflectarrays: Providing multispot coverage with a smaller number of apertures for satellite communications in the K and Ka bands," *IEEE Antennas and Propagation Magazine*, Vol. 61, No. 5, 77–86, Oct. 2019, doi: 10.1109/MAP.2019.2932311.
151. Martinez-de-Rioja, D., R. Florencio, E. Martinez-de-Rioja, M. Arrebola, J. A. Encinar, and R. R. Boix, "Dual-band reflectarray to generate two spaced beams in orthogonal circular polarization by variable rotation technique," *IEEE Transactions on Antennas and Propagation*, Vol. 68, No. 6, 4617–4626, Jun. 2020, doi: 10.1109/TAP.2020.2975294.
152. Zhang, M., et al., "Design of novel reconfigurable reflectarrays with single-bit phase resolution for Ku-band satellite antenna applications," *IEEE Transactions on Antennas and Propagation*, Vol. 64, No. 5, 1634–1641, May 2016, doi: 10.1109/TAP.2016.2535166.
153. Martinez, I., A. H. Panaretos, and D. H. Werner, "Reconfigurable ultrathin beam redirecting metasurfaces for RCS reduction," *IEEE Antennas and Wireless Propagation Letters*, Vol. 16, 1915–1918, 2017, doi: 10.1109/LAWP.2017.2686779.
154. Ren, L.-S., Y.-C. Jiao, F. Li, J.-J. Zhao, and G. Zhao, "A dual-layer T-shaped element for broadband circularly polarized reflectarray with linearly polarized feed," *IEEE Antennas and Wireless Propagation Letters*, Vol. 10, 407–410, 2011.
155. Chaharmir, M. R., J. Shaker, M. Cuhaci, and A. Sebak, "Circularly polarised reflectarray with cross-slot of varying arms on ground plane," *Electronics Letters*, Vol. 38, No. 24, 1492–1493, Nov. 2002.
156. Wu, G.-B., S.-W. Qu, S. Yang, and C. H. Chan, "Broadband, single-layer dual circularly polarized reflectarrays with linearly polarized feed," *IEEE Transactions on Antennas and Propagation*, Vol. 64, No. 10, 4235–4241, Oct. 2016, doi: 10.1109/TAP.2016.2593873.
157. Momeni Hasan Abadi, S. M. A. and N. Behdad, "Broadband true-time-delay circularly polarized reflectarray with linearly polarized feed," *IEEE Transactions on Antennas and Propagation*, Vol. 64, No. 11, 4891–4896, Nov. 2016, doi: 10.1109/TAP.2016.2596900.
158. Kaddour, A.-S., et al., "A foldable and reconfigurable monolithic reflectarray for space applications," *IEEE Access*, Vol. 8, 219355–219366, 2020, doi: 10.1109/ACCESS.2020.3042949.
159. Su, W., W. Luo, Z. Nie, W.-W. Liu, Z.-H. Cao, and Z. Wang, "A wideband folded reflectarray antenna based on single-layered polarization rotating metasurface," *IEEE Access*, Vol. 8, 158579–158584, 2020, doi: 10.1109/ACCESS.2020.3019822.
160. Abdollahvand, M., K. Forooraghi, J. A. Encinar, Z. Atlasbaf, and E. Martinez-de-Rioja, "A 20/30 GHz reflectarray backed by FSS for shared aperture Ku/Ka-band satellite communication antennas," *IEEE Antennas and Wireless Propagation Letters*, Vol. 19, No. 4, 566–570, Apr. 2020, doi: 10.1109/LAWP.2020.2972024.
161. Di Renzo, M., et al., "Smart radio environments empowered by reconfigurable intelligent surfaces: How it works, state of research, and road ahead," *IEEE Journal on Selected Areas in Communications*, Vol. 38, No. 11, 2450–2525, 2020.
162. Liaskos, C., S. Nie, A. Tsioliaridou, A. Pitsillides, S. Ioannidis, and I. Akyildiz, "A novel communication paradigm for high capacity and security via programmable indoor wireless environments in next generation wireless systems," *Ad Hoc Networks*, Vol. 87, 1–16, May 2019,

doi: 10.1016/j.adhoc.2018.11.001.

163. Arun, V. and H. Balakrishnan, "RFocus: Beamforming using thousands of passive antennas," *17th USENIX Symposium on Networked Systems Design and Implementation*, 17, Feb. 2020.
164. Roberts, J., K. L. Ford, and J. M. Rigelsford, "Secure electromagnetic buildings using slow phase-switching frequency-selective surfaces," *IEEE Transactions on Antennas and Propagation*, Vol. 64, No. 1, 251–261, Jan. 2016, doi: 10.1109/TAP.2015.2499773.
165. Tan, X., Z. Sun, J. M. Jornet, and D. Pados, "Increasing indoor spectrum sharing capacity using smart reflect-array," *2016 IEEE International Conference on Communications (ICC)*, 1–6, May 2016, doi: 10.1109/ICC.2016.7510962.
166. "DOCOMO conducts World's first successful trial of transparent dynamic meta-surface," NTT DoCoMo, Inc., Tokyo, Japan, Jan. 17, 2020. [Online]. Available: https://www.nttdocomo.co.jp/english/info/media_center/pr/2020/0117_00.html#:∼:text=TOKY-O%2C%20JAPAN%2C%20January%2017%2C,28%20GHz%205G%20radio%20signals, Accessed on: May 12, 2021.
167. Black, E. J., "Holographic beam forming and MIMO," Pivotal Commware, Inc., Kirkland, WA, USA, Jan. 17, Oct. 2018. [Online]. Available: https://pivotalcommware.com/technology/, Accessed on: May 12, 2021.
168. Pivotal Staff, "Holographic beam forming and phased arrays," Pivotal Commware, Inc., Kirkland, WA, USA, 2019. [Online]. Available: https://pivotalcommware.com/technology/, Accessed on: May 12, 2021.
169. Samaiyar, A., A. H. Abdelrahman, L. B. Boskovic, and D. S. Filipovic, "Extreme offset-fed reflectarray antenna for compact deployable platforms," *IEEE Antennas and Wireless Propagation Letters*, Vol. 18, No. 6, 1139–1143, Jun. 2019, doi: 10.1109/LAWP.2019.2911019.
170. Mei, P., S. Zhang, and G. F. Pedersen, "A low-cost, high-efficiency and full-metal reflectarray antenna with mechanically 2-D beam-steerable capabilities for 5G applications," *IEEE Transactions on Antennas and Propagation*, Vol. 68, No. 10, 6997–7006, Oct. 2020, doi: 10.1109/TAP.2020.2993077.
171. Wu, G., Y. Zeng, K. F. Chan, B. Chen, S. Qu, and C. H. Chan, "High-gain filtering reflectarray antenna for millimeter-wave applications," *IEEE Transactions on Antennas and Propagation*, Vol. 68, No. 2, 805–812, Feb. 2020, doi: 10.1109/TAP.2019.2943432.
172. An, W., L. Xiong, S. Xu, F. Yang, H. Fu, and J. Ma, "A Ka-band high-efficiency transparent reflectarray antenna integrated with solar cells," *IEEE Access*, Vol. 6, 60843–60851, 2018, doi: 10.1109/ACCESS.2018.2875359.
173. Chen, Y.-S., Y.-H. Wu, and C.-C. Chung, "Solar-powered active integrated antennas backed by a transparent reflectarray for CubeSat applications," *IEEE Access*, Vol. 8, 137934–137946, 2020, doi: 10.1109/ACCESS.2020.3012133.
174. Yekan, T. and R. Baktur, "Conformal integrated solar panel antennas: Two effective integration methods of antennas with solar cells," *IEEE Antennas and Propagation Magazine*, Vol. 59, No. 2, 69–78, Apr. 2017, doi: 10.1109/MAP.2017.2655577.
175. Jenkins, R. P., et al., "A low-power tunable frequency selective surface for multiplexed remote sensing," *IEEE Access*, Vol. 9, 58478–58486, 2021, doi: 10.1109/ACCESS.2021.3070715.